THE EFFECT OF FLUX AND GRAVITATIONAL FORCES ON MISCIBLE DISPLACEMENT IN A THIN HOMOGENEOUS BED

A Thesis

Submitted to the Graduate Faculty of the
Louisiana State University and
Agricultural and Mechanical College
in partial fulfillment of the
requirements for the degree of
Master of Science

in

The Department of Petroleum Engineering

by
Walid Jubran Esmail
B.S., Louisiana State University, 1971
August, 1973

ACKNOWLEDGMENT

The author is gratefully indebted to Dr. Oscar K. Kimbler, Professor of Petroleum Engineering, under whose guidance and supervision this work was accomplished.

Likewise, special words of appreciation are extended to Dr. Raphael G. Kazmann, Professor of Civil Engineering, Dr. William R. Holden, Professor of Petroleum Engineering, Dr. William J. Bernard and Dr. Adam T. Bourgoyne, Assistant Professors of Petroleum Engineering and the remainder of the Petroleum Engineering Department for their constructive comments and suggestions.

The help of Mr. Walter R. Whitehead, Ph.D. candidate in Civil Engineering, in computer programing and Mrs. Mary Matens for typing the thesis, is gratefully acknowledged.

Finally, to my parents, whose help and encouragement will never be forgotten, I humbly dedicate this work.

This study was financed by a grant from the Louisiana Water Resources Research Institute under P.L. 88-379, Federal Office of Water Resources Project A-027-LA.

TABLE OF CONTENTS

TABLE OF CONTENTS (continued)

LIST OF TABLES

LIST OF FIGURES

ABSTRACT

The feasibility of utilizing horizontal saline aquifers for cyclic storage of fresh waters has been established by previous investigators. In addition, it was found that the recovery efficiency in a dipping mini-aquifer, incorporating a semi-circular isopotential as the outer boundary, is less than that in the horizontal case.

The present study experimentally investigates gravitational effects in a dipping semi-bounded mini-aquifer and also incorporates the effect of pre-existing groundwater movement (flux) in both horizontal, and dipping systems. In all cases studied, the direction of the flux was parallel to the closed boundary of the system. In the horizontal system, flux always reduced recovery efficiency. In dipping systems, flux may either improve or reduce recovery efficiency. Use of a closed boundary in the present study had little effect on recovery efficiencies presently reported as long as the boundary was not closely approached by the injected fluid.

A mathematical model was developed for a three dimensional system to predict the recovery efficiency for horizontal and dipping systems with, or without flux. This model employs a streamline tracking procedure and incorporates mixed zone length and an approximation of frontal

laydown. Recovery efficiencies predicted by the model were compared to those obtained in 21 experimental runs. Good agreement was observed in all horizontal runs and in dipping systems in which no flux was present. Less agreement was shown in dipping systems in which flux was present. In such systems the agreement was good when flux rates were moderate and poor when flux rates were high.

Results of this study are applicable to miscible displacement operations where a density difference exists between the native and the injected fluids in horizontal and dipping systems. Subsurface waste disposal and the secondary recovery operations in the petroleum industry are examples of such applications.

CHAPTER I

INTRODUCTION

The possibility of underground fresh water storage in saline aquifers has gained the attention of several investigators: Cederstrom, 1947; Moulder and Frazor, 1957; Esmail, 1966; Green and Cox, 1966; Esmail and Kimbler, 1967; Kumar and Kimbler, 1970; Francis, 1970; Painter, 1971; and Gelhar, 1972. In many areas, such as flat coastal regions and urban centers, the cost of surface storage facilities is economically unattractive because of the high cost of either tankage or land. If suitable storage aquifers could be used, the cost of storing large quantities of fresh water would be tremendously reduced. It has been estimated that in one coastal urban area the annual cost of storing 120 million gallons of water underground might be only $25,000. Assuming a 6% interest rate and a 50 year tank life, the annual cost of storing this quantity in steel tanks would be about $760,000.[1]

In recent studies, of which this study is a continuation, investigators have suggested that such a process is technically feasible under specified conditions. Esmail,[2] conducting experiments on pie-shape thin sandstone mini-aquifer, concluded that such a process is feasible, from a recovery point of view, for aquifers of

low permeability, utilizing high flow rates, and short storage times. Based on similar experiments on a thicker mini-aquifer, Kumar and Kimbler[3] reported that use of thin formations that possess low aquifer water salinities would result in high recovery efficiencies. Their work showed that the recovery efficiency improves with an increase in the number of injection-production cycles. Moreover, their computer model showed that stratification improves the recovery efficiency in the absence of cross flow. Painter[4] worked with a thin three dimensional mini-aquifer incorporating a circular isopotential (the model represented half a system). His findings showed that the recovery efficiency of cyclic injection and production into an aquifer possessing dip is less than in a horizontal system of identical hydrologic properties. This difference is mainly related to the density difference and the dip angle. An important conclusion drawn from his work was that an injected bubble maintains its original configuration during gravity migration in the absence of injection and production.

The prevailing movement of underground water changes the recovery efficiency of a subsurface storage project. This movement may be either natural or the result of production of wells elsewhere in the same aquifer in which fresh water is being stored. Depending on the rate of movement, the configuration of the injected water will

be altered to some extent, and consequently, the recovery efficiency will be reduced.

The objective of this research, therefore, was to study the gravitational effects resulting from density difference between the native and the injected fluids and the effects of pre-existing ground water movement in horizontal and dipping aquifers. In addition, it sought to combine the results of previous studies into a single mathematical model to predict the recovery efficiency for a single well system under a variety of hydrologic conditions.

Results of this study, as well as the previous studies also may be applicable to underground waste disposal, natural gas storage in aquifers with cushion gas, and secondary recovery operations in the petroleum industry.

CHAPTER II

REVIEW OF THEORY AND PREVIOUS INVESTIGATIONS

The process of storing fresh water in saline aquifers is an application of miscible displacement in porous media. A brief review of the theory and of previous investigations are presented below to outline and elucidate the most important phenomena affecting miscible displacement.

2.1 Molecular Diffusion and Convective Dispersion

If two miscible fluids of different composition are in contact, a transfer of molecules will result. As time passes, the random movement of molecules creates a mixed zone between the two fluids; that is the two fluids diffuse into one another. The mathematical description of this phenomenon is given by Fick's first and second laws of diffusion.

If miscible fluids flow through porous medium, additional mixing results from velocity variations which cause concentration gradients. This additional mixing is referred to in this thesis as dispersion. Dispersion falls into two categories: if it acts in the direction of flow, it is referred to as longitudinal dispersion; if it acts perpendicular to the direction of flow, it is transverse dispersion. The latter occurs in the presence of large difference in fluid composition and is not treated explicitly in this study.

The flow around a single well in an infinite system is radial. For this case, Raimondi et al.[5] formulated a relationship between concentration, distance, and time of injection represented by the differential equation:

$$\frac{\partial C}{\partial t} + \frac{Q}{r}\frac{\partial C}{\partial r} = \left(\frac{\alpha r}{Q} + \frac{Dr^2}{Q^2}\right)\frac{\partial^2 C}{\partial t^2} \quad \ldots\ldots(2.1)$$

where

C = concentration of injected fluid, fraction

Q = $q/2\pi\phi h$, cm^2/sec (q = volumetric flow rate, cc/sec)

r = radial distance, cm

D = diffusion coefficient in porous media, cm^2/sec

α = longitudinal coefficient of convective dispersion, cm.

These authors present solutions to this equation for both injection and production. These solutions are of the form:

$$C = 0.5\left[1 - \text{erf}[(Qt - 0.5\ r^2)/f(r)]\right] \quad \ldots(2.2)$$

where

$$[f(r)]^2 = 4\ \alpha\ r^3/3 + D\ r^4/Q.$$

The coefficient of convective dispersion α is defined in terms of the inhomogeneity factor σ and the mean particle diameter dp as,

$$\alpha = \sigma^2 dp \quad \ldots\ldots\ldots(2.3)$$

These solutions were verified experimentally by Esmail and Kimbler for two injection and production half cycles. This treatment of longitudinal dispersion was utilized in the present study.

2.2 Gravity Segregation

If two fluids with different densities are in contact, the more dense fluid underruns the less dense fluid and spreads along the bottom. This is called gravity segregation.

Gravity segregation may be of two types: (1) static and (2) dynamic. The static case involves no bulk flow except that caused by convective currents due to gravity. The dynamic case, on the other hand, takes place during bulk flow. However, in their investigation, Esmail and Kimbler postulated and Kumar[6] later verified, that miscible fluids will have equal dynamic and static segregation for a unit mobility ratio.

In the static case, Kidder, Dietz, and Gardner et al.[7] investigated the tilt of the interface with respect to the vertical between two miscible fluids. Esmail and Kimbler[8] suggested that the density gradient S, defined as the ratio of the density difference to the length of the mixed zone, will tend to retard the rate of inclination of the boundary. They formulated an expression for the projection of the interface as:

$$\frac{2y}{h} = f\left[\frac{K_H\, g\, \Delta\rho t}{\phi \bar{\mu}\, h}\right]\left[\frac{(\bar{\mu})^{2/3}\, S}{(\sigma\rho)^{5/3}\, g^{1/3}}\right] \quad \ldots\ldots (2.4)$$

where

f = some function of the quantities in the brackets.

From experimental data obtained on linear systems, Esmail

and Kimbler obtained a two part curve, a straight line and a parabola, which they corrected for radial geometry and used in calculating gravity segregation during the storage process. Kumar found Equation (2.4) to be applicable for both static and dynamic gravity segregation.

2.3 Gross Fluid Movement in Dipping Systems

In a horizontal system, the difference in density of two fluids acts only as described in Section 2.2. In dipping systems, however, an additional effect is present. This is the tendency for gross migration of the less dense fluid in the updip direction. This latter effect is difficult to describe analytically. The updip and down-dip positions of the injected fluid have been analytically evaluated by Painter as:

$$X_u = \frac{q_i t}{2A\phi} + 4.94 \times 10^{-7} \frac{k\,\Delta\rho\, g\, \text{Sin}\,\alpha\, q_i t^2}{\mu L A \phi^2} \quad \ldots (2.5)$$

$$X_d = \frac{q_i t}{2A\phi} - 4.94 \times 10^{-7} \frac{k\,\Delta\rho\, g\, \text{Sin}\,\alpha\, q_i t^2}{\mu L A \phi^2} \quad \ldots (2.6)$$

where

X_u = up-dip frontal location at t, cm

X_d = down-dip frontal location at t, cm

q_i = injection rate, cc/sec

A = total cross-sectional area, cm^2

L = total length, cm

t = time, sec

ϕ = porosity

g = gravitational acceleration, cm/sec^2

k = permeability, darcies

$\Delta\rho$ = density difference, gm/cc

α = dip angle, degrees

μ = viscosity, cp

Assumptions inherent in the above equations are:

(1) Piston-like displacement (No mixed zone, and front perpendicular to direction of flow)

(2) Fluids of small and constant compressibility

(3) Homogeneous and isotropic porous medium of finite length, L

(4) Breakthrough has not occured in either direction.

Painter found good agreement between these equations and experimental data taken on a linear model.

In the linear system the displaced fluid simply moves linearly toward the ends of the system which are held as isopotentials. In the dipping radial system, however, there must be a movement, or circulation, of displaced fluid around the mass of injection fluid. This circulation, together with the fact that the streamlines resulting from injection or production are constantly changing in strength and direction, makes an analytical description of the radial system much more complex. In view of the complexity of the problem, Painter resorted to an experimental technique using a large (230 cm x 110 cm) flow model only 1.0 cm in thickness. The model contained a single well surrounded by a semicircular isopotential located 105 cm from the well. He used data from this

model together with the concepts relating to the linear system to develop a streamline tracking procedure with which he hoped to predict recovery efficiency in the radial system. This was accomplished in the following manner.

Taking the first derivative of Equations (2.5) and (2.6) gives the velocities in the respective directions as:

$$\frac{dX_u}{dt} = \vec{V}_u = \frac{q_i}{2A\phi} + 9.88 \times 10^{-7} \frac{k\ \Delta\rho\ g\ \text{Sin}\ \alpha\ q_i t}{\mu LA\phi^2} \qquad (2.7)$$

$$\frac{dX_d}{dt} = \vec{V}_u = \frac{q_i}{2A\phi} - 9.88 \times 10^{-7} \frac{k\ \Delta\rho\ g\ \text{Sin}\ \alpha\ q_i t}{\mu LA\phi^2} \qquad (2.8)$$

The first term in both equations, $\frac{q_i}{2A\phi}$, is the actual velocity in a horizontal system or in a tilted system with no density difference. The second term is the same except for the sign and can be rewritten as:

$$9.88 \times 10^{-7} \frac{k\ \Delta\rho\ g\ \text{Sin}\ \alpha}{\mu\phi} \left[\frac{q_i t}{AL\phi}\right]^n \quad . \quad . \quad . \quad . (2.9)$$

where n = 1.0. The total velocity is the sum of the actual velocity and the gravity component. For a half radial system, the total velocity vector is given by:

$$\vec{V}_x = \frac{q}{\pi h\phi} \left(\frac{x}{x^2 + y^2}\right) + 9.67 \times 10^{-4} \frac{k\ \Delta\rho\ \text{Sin}\ \alpha}{\mu\phi} \left[\frac{2qt}{\pi\ r_e^{\ 2}\ h\phi}\right]^n \qquad (2.10)$$

where

$\left[\frac{2qt}{\pi\ r_e^{\ 2}\ h\phi}\right]^n$ = a ratio of the cumulative volume of injected fluid at any time to total pore volume, dimensionless.

In a linear system, the fluid is restricted to move parallel to the boundaries; in radial systems, however, circulation of fluid around the perphery of the injected "bubble" takes place. This difference in fluid movement brings about a change in the value of "n". From a series of runs using a mini-aquifer with circular isopotential, Painter found an emperical value of "n" of 0.17. This value, which is also used in the present study, was substituted in the velocity vector $\vec{V}_x$ which was used in the computer program to calculate recovery efficiency.

Although the program was written to track as many streamlines as desired, only that streamline along the direction of dip (i.e., that streamline which will be responsible for first breakthrough into the well) was used in predicting recovery efficiency. The computational technique was only moderately successful in predicting experimentally observed recovery efficiencies, in some cases giving good agreement while in others the agreement left much to be desired. The approach, however, appears sound and has formed the basis for the treatment used in the present study.

CHAPTER III

EXPERIMENTAL PROCEDURE

The radial mini-aquifer and peripheral equipment used by Painter are shown schematically in Figure 3.1. The mini-aquifer was constructed of an epoxy-sand mixture and measured 230 cm x 110 cm x 1.0 cm. A detailed description of the construction has been given by Painter. It is supported by a 1/2" x 4' x 8' transparent acrylic sheet fastened to a 2" x 4" stock frame. The support legs are 6" x 6" redwood stock secured to the frame by 1/2" x 4' rods. The structure can be positioned to any angle desired by placing a rod through the taller support legs. Illumination, for photographic and visual purposes, is provided by fluorescent light fixtures suspended beneath the acrylic sheet. However, the capacitance cell used in this study was installed on the wellbore.

As used by Painter, the apparatus consists of one half of the radial system shown in Figure 3.2. This simplification is possible because of the symmetry of the system. The present study utilized the same model except that the circular isopotential was removed, leaving only a slot at each end, as shown in Figure 3.1, to serve as isopotentials. These slots provided the means for introducing flux (prevailing fluid movement) into the system when desired. Pressure on the model, which ranged between

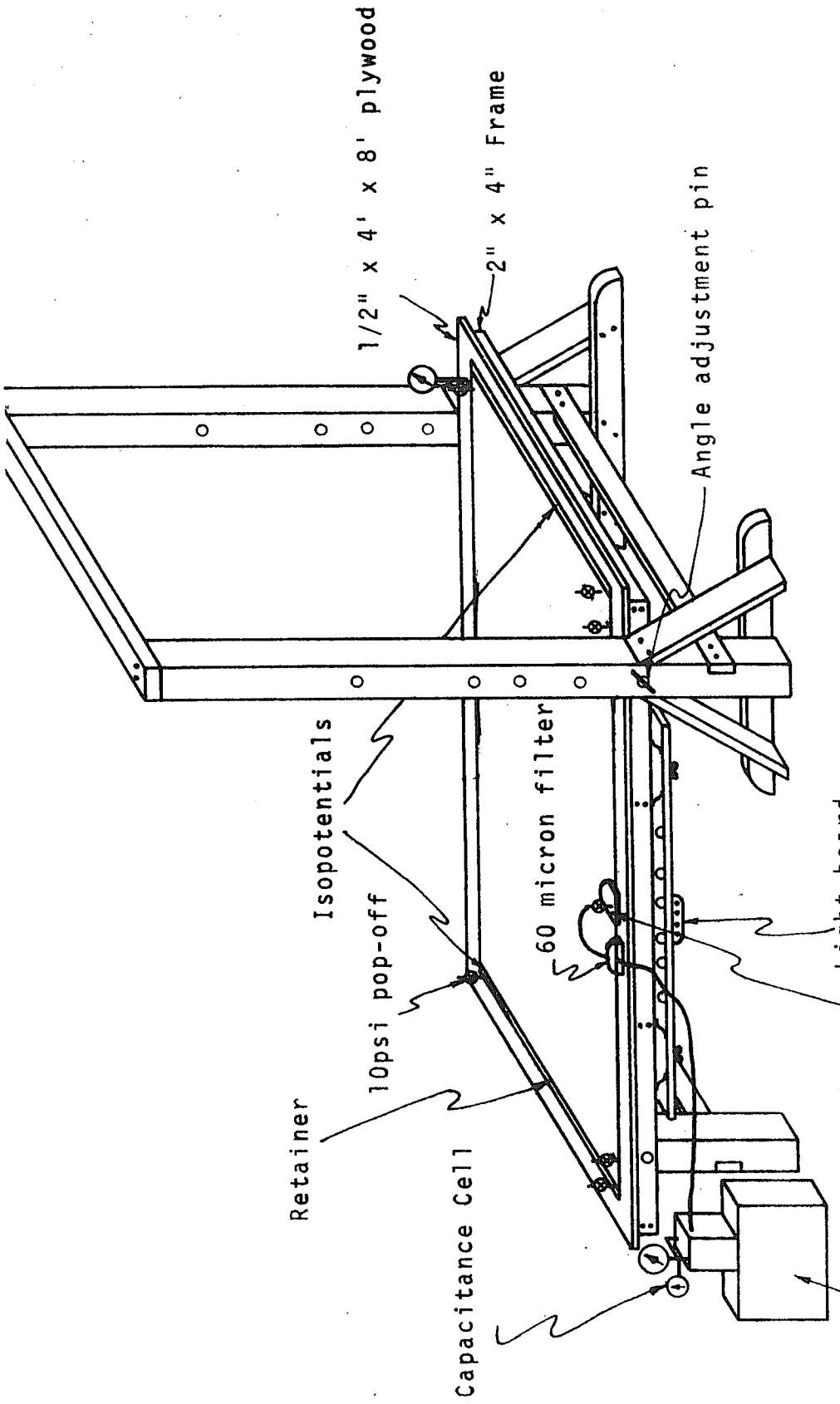

FIGURE 3-1 SCHEMATIC DIAGRAM OF THE MINI-AQUIFER AND SUPPORTING STRUCTURE. (AFTER PAINTER)

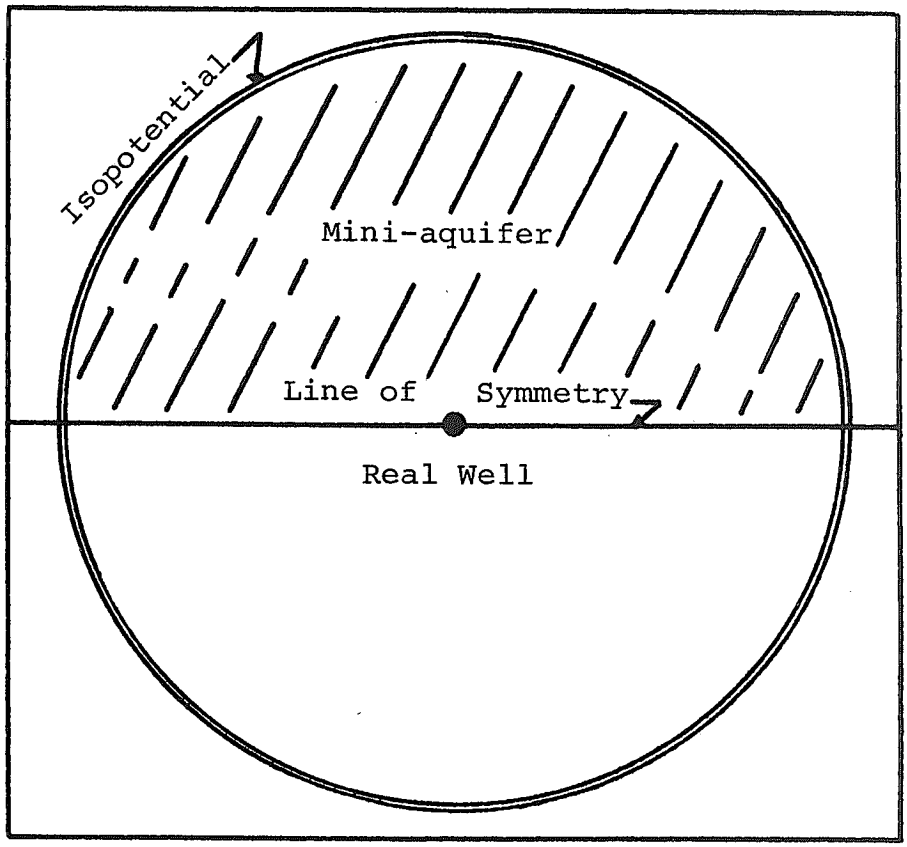

FIGURE 3.2 PLAN VIEW OF MINI-AQUIFER AND THE ISOPOTENTIAL BOUNDARY USED BY PAINTER

2.0 to 3.5 psi, is exerted by the weight of a column of fluid from a reservoir seven feet above the surface of the model.

The change in the outer boundaries of the model from a circular to a semi-longitudinal type brought about two no-flow boundaries for the full system as shown in Figure 3.3. For calculation purposes, introduction of image wells on both sides of the model are necessary to produce the effect of the no flow boundaries. Such image wells are sketched in Figure 3.3. Because of the symmetry involved, only half the system is required as shown by the cross hatched area of the figure.

The first runs were made under conditions which duplicated those of selected runs by Painter. The purpose was to test whether the changes in either the isopotentials or the outer boundaries affected in any way the shape of the displacement fronts or the recovery efficiency. The second set tested the effect of gravitational forces and flux on recovery efficiency for both horizontal and dipping systems. Among the parameters studied were the density difference, injection and production rates, flux rates, injection times, and angles of dip. Throughout this study, in any given run, injection and production rates were kept equal.

In all cases, the model was initially saturated with a mixture of 45% soltrol and 55% naphtha by volume. The injected fluid consisted basically of this same fluid

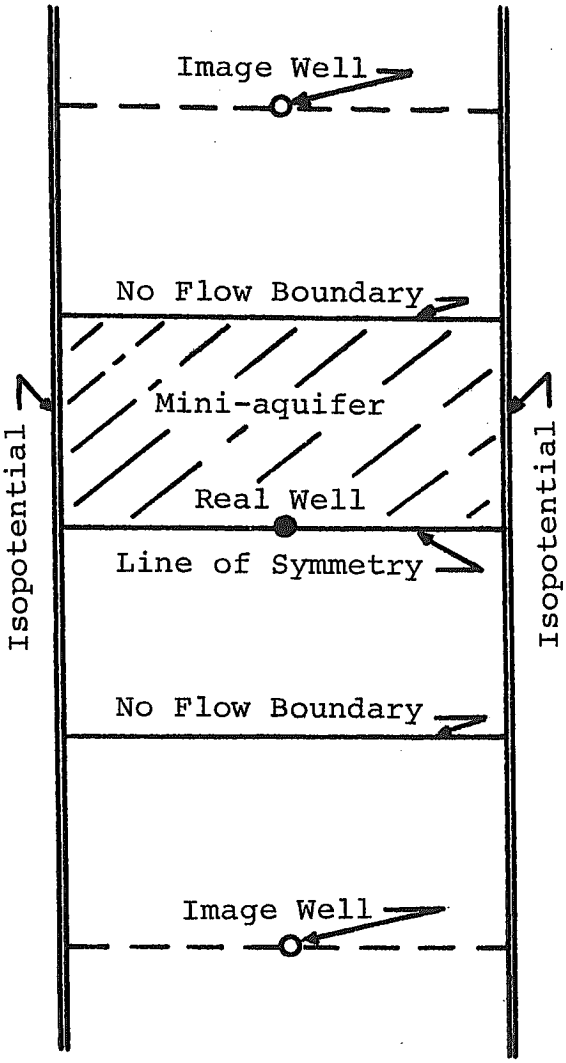

FIGURE 3.3 PLAN VIEW OF MINI-AQUIFER AND THE ISOPOTENTIAL BOUNDARY USED IN THE PRESENT STUDY

together with small quantities of dye and about 1.5% iodobenzene by volume. Carbon tetrachloride was used to vary the density. The ratio of soltrol and naphtha is such that the mixture has a viscosity which is equal to that of carbon tetrachloride. When carbon tetrachloride is added to the injected fluid, the viscosity of the injected fluid and that of the reservoir (original saturating fluid) fluid will be identical, thus maintaining a unit mobility ratio. The effect of adding small quantities of the dye and iodobenzene makes an insignificant change in the viscosity of the injected fluid.

The purpose of the dye is to make the progress of the injected front visible. The purpose of the iodobenzene is to alter the dielectric properties of the injected fluid from those of the reservoir fluid. During the production half cycle, the change in dielectric constant of the produced fluid is sensed by a capacitance cell connected to a Chemical Oscillometer. When the Oscillometer detects a change in the capacitance, this indicates that the reservoir fluid is being produced; that is, breakthrough has occurred.

It will be noted that analog fluids are used throughout the study and that the more dense fluid is used as the injection, or stored, fluid. Such fluids are much more desirable for experimental use than fresh and saline water in that much better control of properties is possible. For example, a wide range of density difference can be

obtained without introducing any differences in viscosity. The more dense fluid is used as the injected fluid because it is easier and more economical to prepare.

Constant rate piston pumps are used for injection and production. The injection half cycle proceeds for the desired time; then the pumps are set on production until breakthrough. The recovery efficiency is taken to be the ratio of the production time until breakthrough to the injection time. The position of the leading edge of the injected fluid front was marked on the surface of the mini-aquifer. These outlines were later transferred to tracing paper. After each run, the injected fluid was completely flushed out to prepare the apparatus for another run.

In those experiments involving flux the pumps used to provide flux were attached to one end of the model, while the other isopotential remained attached to the overhead fluid reservoir. The fluid used to produce flux was of the same composition as the reservoir fluid. The potential gradient due to flux can be readily changed simply by changing the pump rate.

Well and flux pumps start the injection half cycle simultaneously. At the end of the injection time, the pumps at the well are changed to production while the pumps providing flux continue to inject fluid; that is the flux continues through the two half cycles. Recovery efficiency is determined as before. Frontal positions

were traced on the surface of the model and subsequently retraced on tracing paper.

Two cycle runs were made as follows: at the end of the first production half cycle (i.e., at breakthrough), the pumps at the well are returned to injection for the second injection half cycle. At the end of the injection period, these pumps are set on production for the second production half cycle. Throughout the run, the pumps providing flux are on injection. In a two cycle run, two recovery efficiencies (one for each cycle) are obtained.

Using the general technique described above, the following types of experiments were performed:

(1) Model horizontal, no flux

(2) Model horizontal with flux

(3) Model dipping, no flux

(4) Model dipping with flux

The purpose of the various types of runs was to test the validity of the individual portions of the mathematical model described in Chapter V. Results of the experiments are discussed in Chapter IV.

CHAPTER IV

EXPERIMENTAL RESULTS

4.1 Results of Runs in Horizontal and Dipping Systems Without Flux

To determine the effect, if any, of the isopotential alterations on the shape of the front and on the recovery efficiency, several horizontal radial runs were made. The density difference was varied for both horizontal and dipping runs; the dip angle was varied for the dipping systems.

For a density difference of less than approximately 0.02 gm/cc, the shapes of the fronts for the horizontal system were somewhat radial during injection and production half cycles for relatively small injected "bubble" as shown in Figures 4.1 and 4.2. These tracings were obtained from Runs 1 and 2 which were made under identical experimental conditions. The tracings showed good reproducibility of frontal shapes. Recovery efficiencies were essentially identical as shown in Table 4.1. The observation that the fronts are essentially radial for this injected volume suggests that the isopotential alteration had no pronounced effect.

To further check the possible effect of the isopotential alteration in the dipping systems, several runs using identical parameters to those of Painter's were

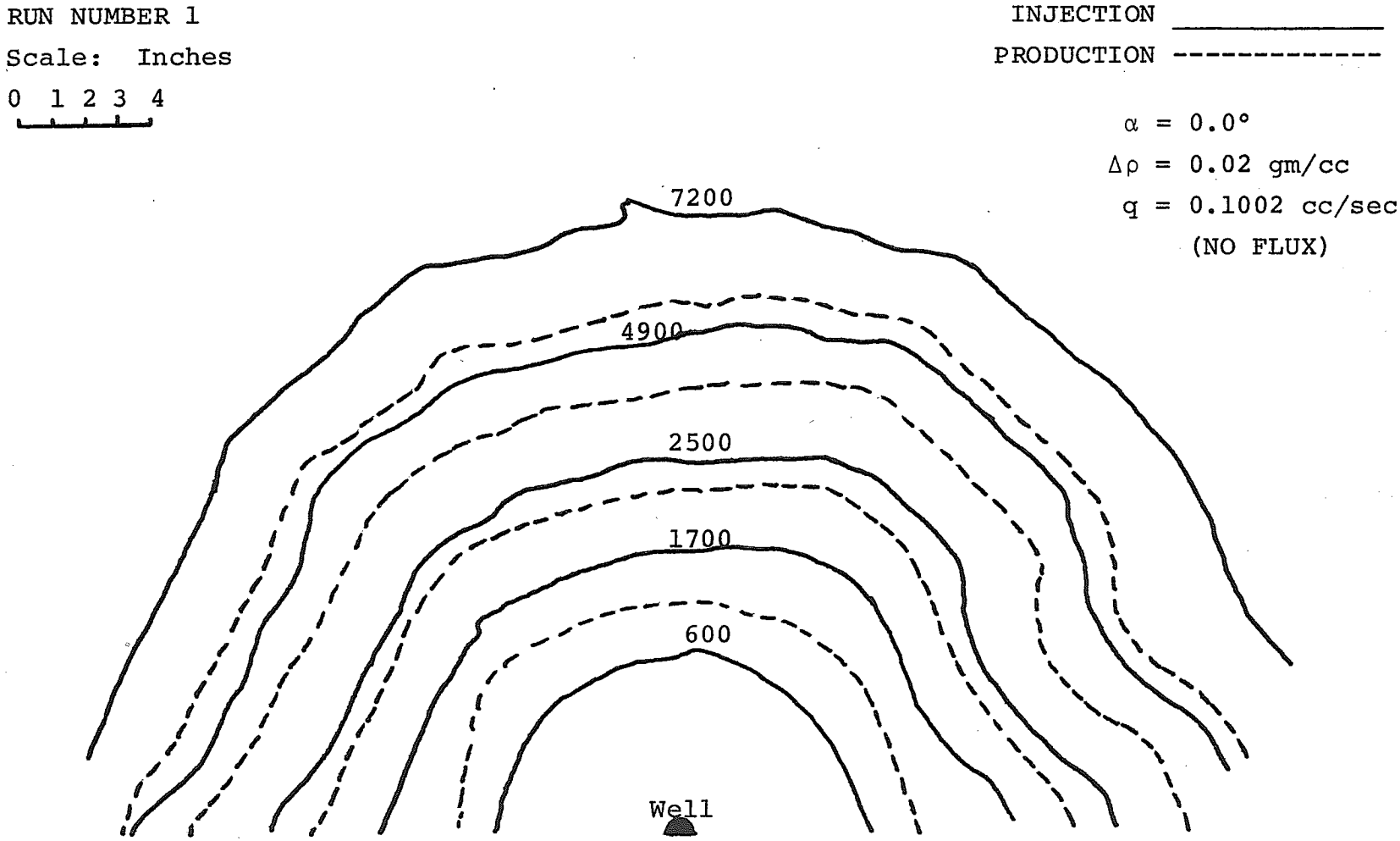

FIGURE 4.1 SELECTED FRONTAL POSITIONS DURING A TYPICAL HORIZONTAL RADIAL DISPLACEMENT

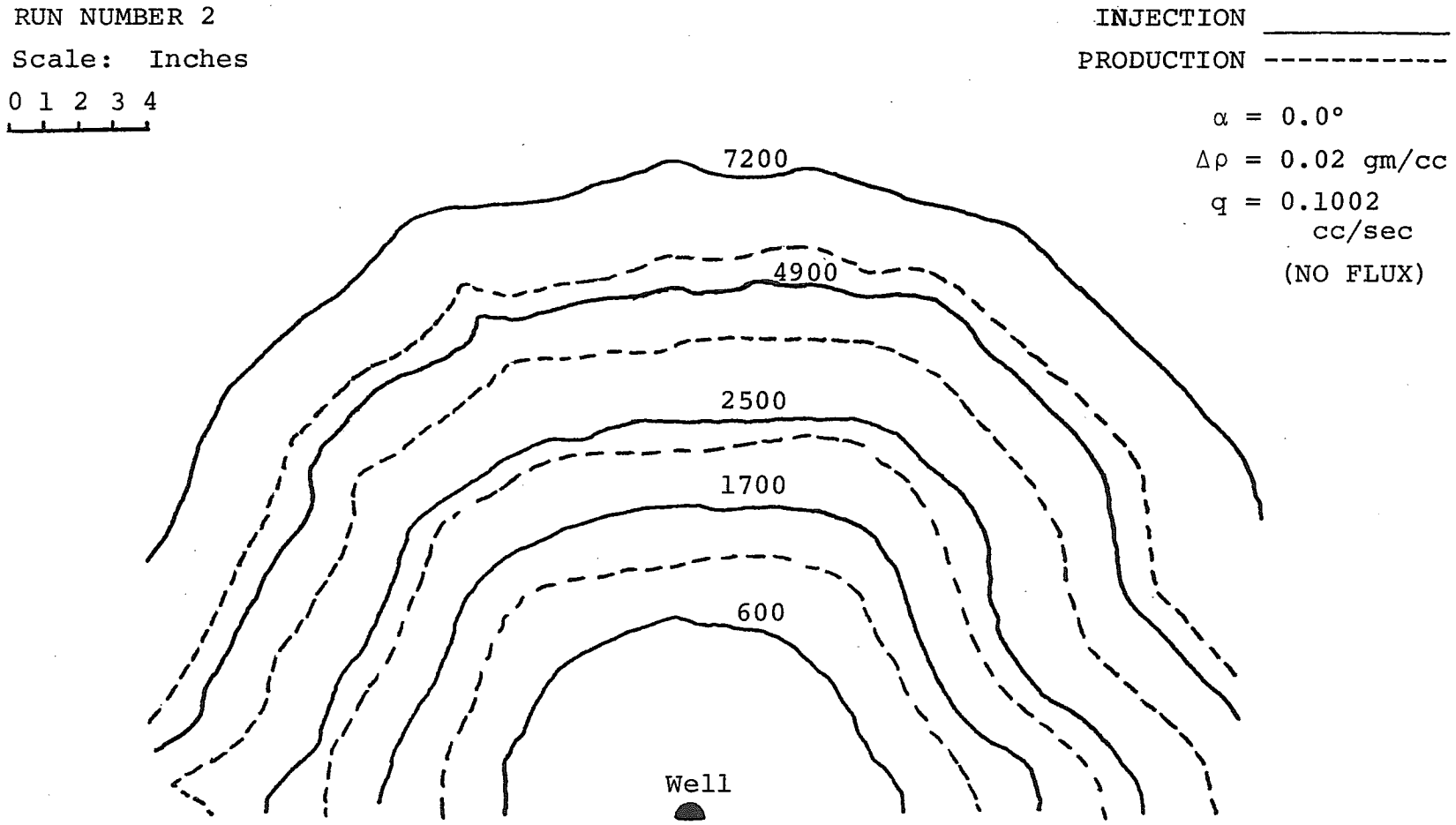

FIGURE 4.2 SELECTED FRONTAL POSITIONS DURING A TYPICAL HORIZONTAL RADIAL DISPLACEMENT

TABLE 4.1

OBSERVED RECOVERY EFFICIENCY FOR
HORIZONTAL RADIAL RUNS WITHOUT FLUX

Run No.	Density Difference gm/cc	Injection and Production Rates cc/sec	Injection Time sec.	Recovery Efficiency %
1	0.02	0.1002	7200	86
2	0.02	0.1002	7230	87

made. For short injection times, the frontal positions were reasonably similar to Painter's as shown in Figure 4.3. However, as the injected volume increased, the fronts flattened in the middle because of the effect of the no flow boundary. The fronts bulged at the ends where the isopotentials do not hinder the advance of the fronts. These effects are apparent in Figure 4.4. The downdip front continued to slide in the direction of dip during the production half cycle.

Surprisingly, the difference in recovery efficiencies due to the change in the positions of the isopotentials was not large as the results in Table 4.2 indicate. Part of this difference may be due to slight differences in the experimental technique and the observation idiosyncrasies of two persons performing similar experiments at different times. The greatest difference in results is shown in Run 6 where Painter used a less accurate technique for detecting breakthrough. Inasmuch as the minor lack of agreement is not consistently in the same direction, it might be appropriate to conclude that the alteration in the isopotential had little adverse effect on the ultimate results of the experiments.

4.2 Results of Runs in Horizontal and Dipping Systems With Flux

Two horizontal runs were made which were identical except that the flux was introduced at opposite ends of

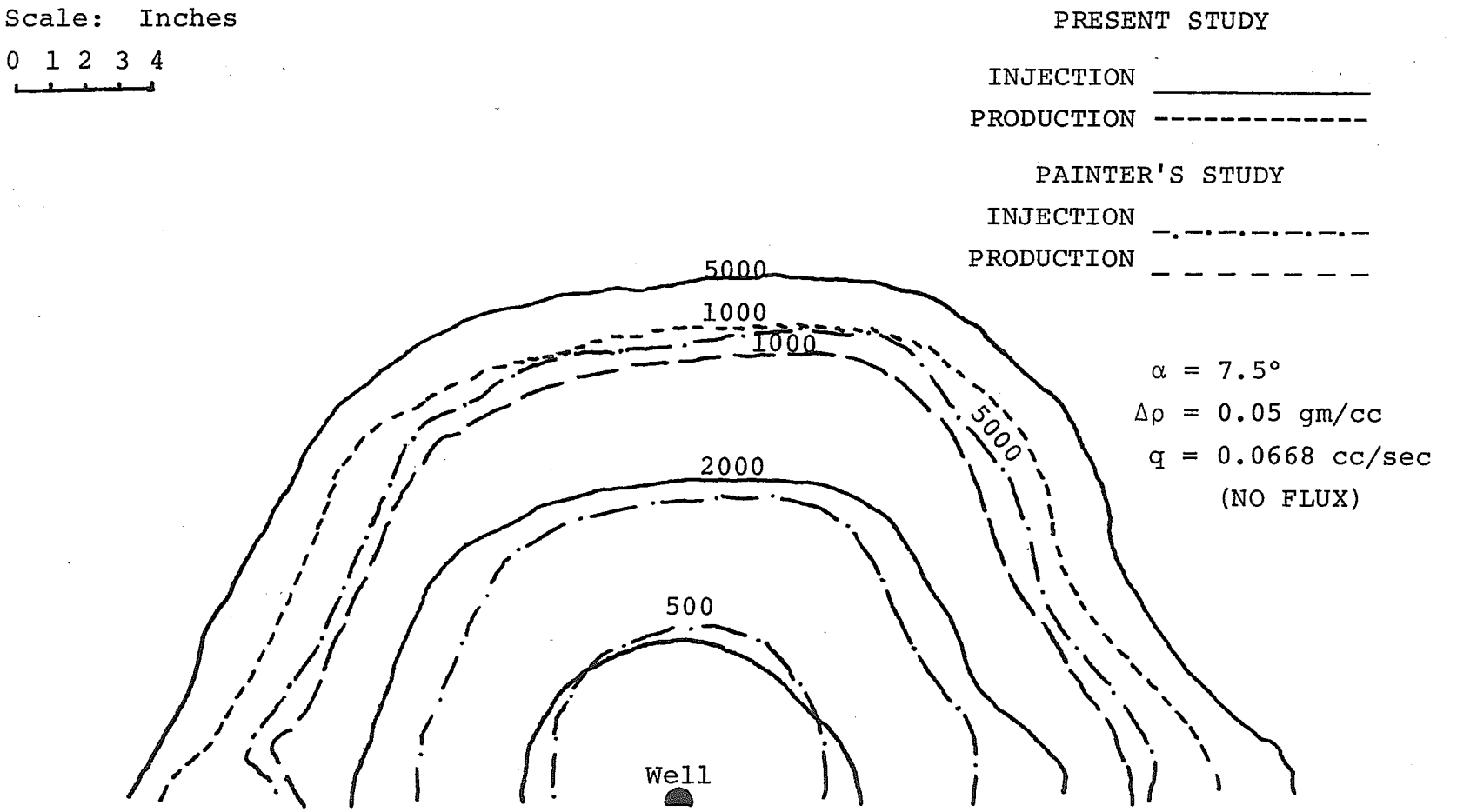

FIGURE 4.3 COMPARISON OF SELECTED FRONTAL POSITIONS FROM RUN 4 OF THE PRESENT STUDY TO THOSE OF PAINTER

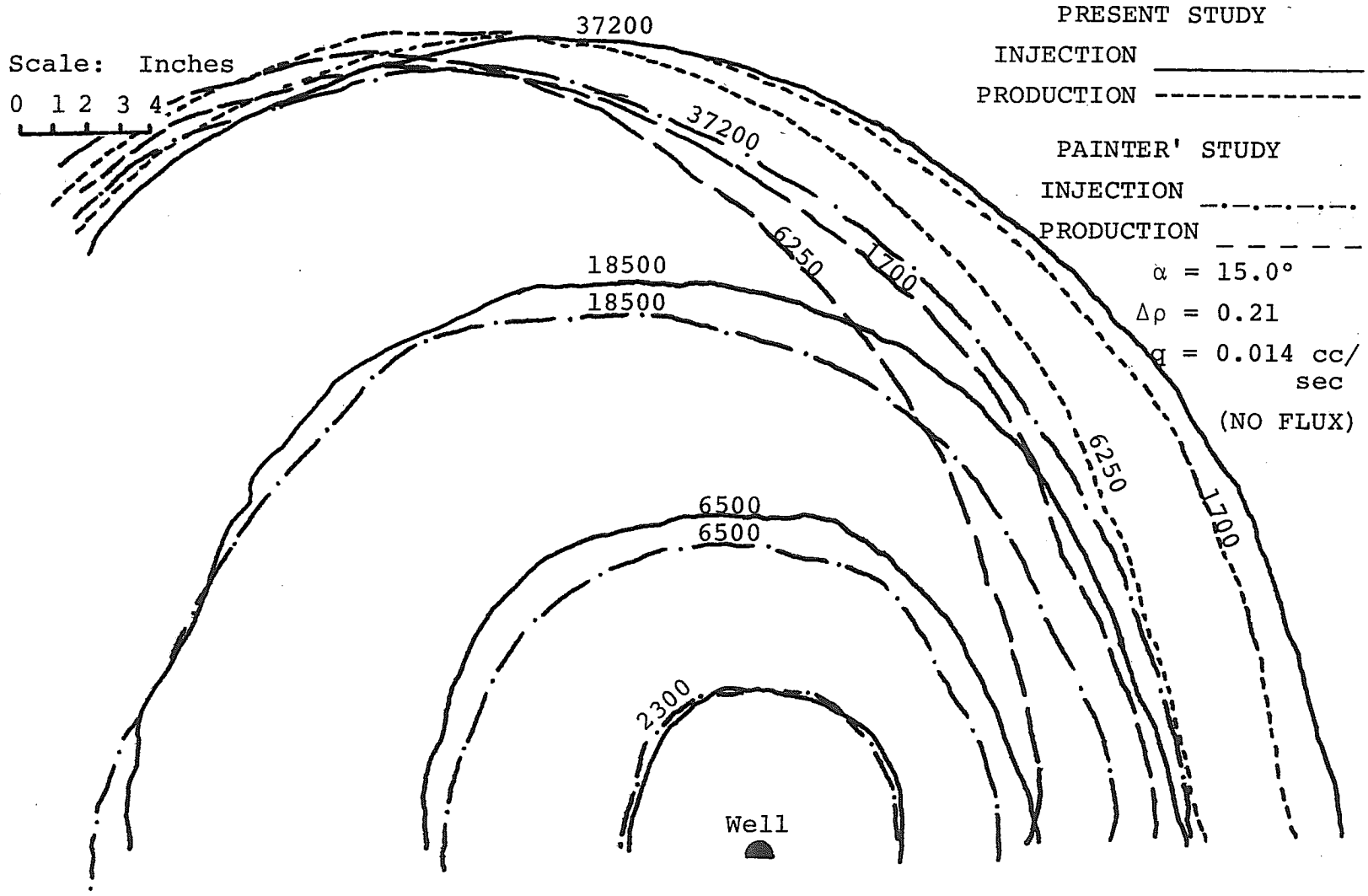

FIGURE 4.4 COMPARISON OF SELECTED FRONTAL POSITIONS FROM RUN 6 OF THE PRESENT STUDY TO THOSE OF PAINTER

TABLE 4.2

COMPARISON OF OBSERVED RECOVERY
EFFICIENCY IN DIPPING SYSTEMS
WITHOUT FLUX

Run No.	Dip Angle degrees	Density Difference gm/cc	Injection and Production Rates cc/sec	Injection Time sec.	Recovery Present Study	Efficiency % Previous Study (Painter)
3	7.5	0.83	0.0264	11400	22	15
4	7.5	0.05	0.0668	5000	82	86
5	15.0	0.05	0.0278	13150	73	68
6	15.0	0.21	0.0140	37200	29	17*
7	30.0	0.21	0.0668	7200	46	**

* Breakthrough Predicted by Pressure Sensor

** No Similar Run by Painter

the model. These were performed to check on the homogeneity of the model and the effects, if any, on the recovery efficiency. The "bubble" injected through the single well exhibited a different configuration and different frontal irregularities in the two cases. However, there was no difference in the recovery efficiency. Consequently, in all other runs with the exception of Run 16, the flux was introduced at the end farthest removed from the angle adjustment pin (see Figure 3.1).

Mathematically, the velocity vector associated with the flux in the "x" direction is described by Darcy's law for linear flow as:

$$\vec{V}_x = - \frac{k}{\mu \phi_D} \Phi_x \quad \ldots\ldots\ldots\ldots (4.1)$$

where

$\vec{V}_x$ = apparent velocity, cm/sec

k = permeability, darcys

μ = viscosity, cp

ϕ_D = displacable porosity, fraction

Φ_x = potential gradient, atmospheres/cm

During injection at the well, the velocity component of the flux in the "x" direction will add vectorially to the velocity component in the "x" direction resulting from injection into the well. Therefore, particles moving along streamlines oriented in the same direction as those resulting from the flux will advance more and those that are moving against the flux will advance less compared to

horizontal no-flux runs. As a result, breakthrough in a horizontal system will always occur along the streamline which acts along the line of symmetry in the direction opposite to the flux. This will invariably lead to a lower recovery efficiency than would have been observed had no flux been present. Results of Run 1 in Table 4.1 and Run 13 in Table 4.3, both of which are horizontal, illustrate this principle.

In some horizontal experiments involving flux, a portion of the front was noticed to reach a state of equilibrium with the flux during the injection half cycle. Figure 4.5 shows fronts during the injection half cycle at different time intervals for Run 11. The point of equilibrium, 18.4 cm to the right of the well, was reached after 7600 seconds of injection. Linear and radial pressures were superimposed both graphically and mathematically to estimate this point of equilibrium. Graphical, observed and computed values were in reasonable agreement as will be shown in Chapter V. The validity of the principle of superposition for these conditions may be justified if the flux is taken to originate at a point source located at infinity.

The effect on the recovery efficiency of various flux rates in both horizontal and dipping systems is shown in Table 4.3. These data when compared with each other and with Run 6 of Table 4.2 indicate that flux may have either a beneficial or detrimental effect. For example,

TABLE 4.3

OBSERVED RECOVERY EFFICIENCY

FOR RADIAL RUNS WITH FLUX*

Run No.	Dip Angle degrees	Density Difference gm/cc	Injection and Production Rates cc/sec	Flux Rate cc/cm^2 - sec	Injection Time sec.	Observed Recovery Efficiency %
8	0.0	0.020	0.1002	7.6×10^{-4}	7200	23
9	0.0	0.020	0.1002	4.3×10^{-4}	7200	37
10	0.0	0.020	0.1002	2.2×10^{-4}	7200	59
11	0.0	0.020	0.0612	6.1×10^{-4}	10500	17
12	0.0	0.017	0.0668	0.84×10^{-4}	7200	50
13	0.0	0.021	0.0668	0.25×10^{-4}	7200	80
14	15.0	0.210	0.0140	0.84×10^{-4}	15000	52
15	15.0	0.220	0.0140	0.84×10^{-4}	25000	46
*16	15.0	0.230	0.0140	0.84×10^{-4}	15000	14
17	30.0	0.215	0.0140	0.84×10^{-4}	15200	20
18	30.0	0.210	0.0140	1.9×10^{-4}	15000	27

* Flux direction is updip in all runs except Run 16 in which it is downdip.

RUN NUMBER 11

Scale: Inches

0 1 2 3 4

INJECTION _____

PRODUCTION ----------

$\alpha = 0.0°$

$\Delta\rho = 0.02$ gm/cc

$q = 0.06$ cc/sec

$q_{FLUX} = 6.1 \times 10^{-4}$ cc/cm^2 - sec

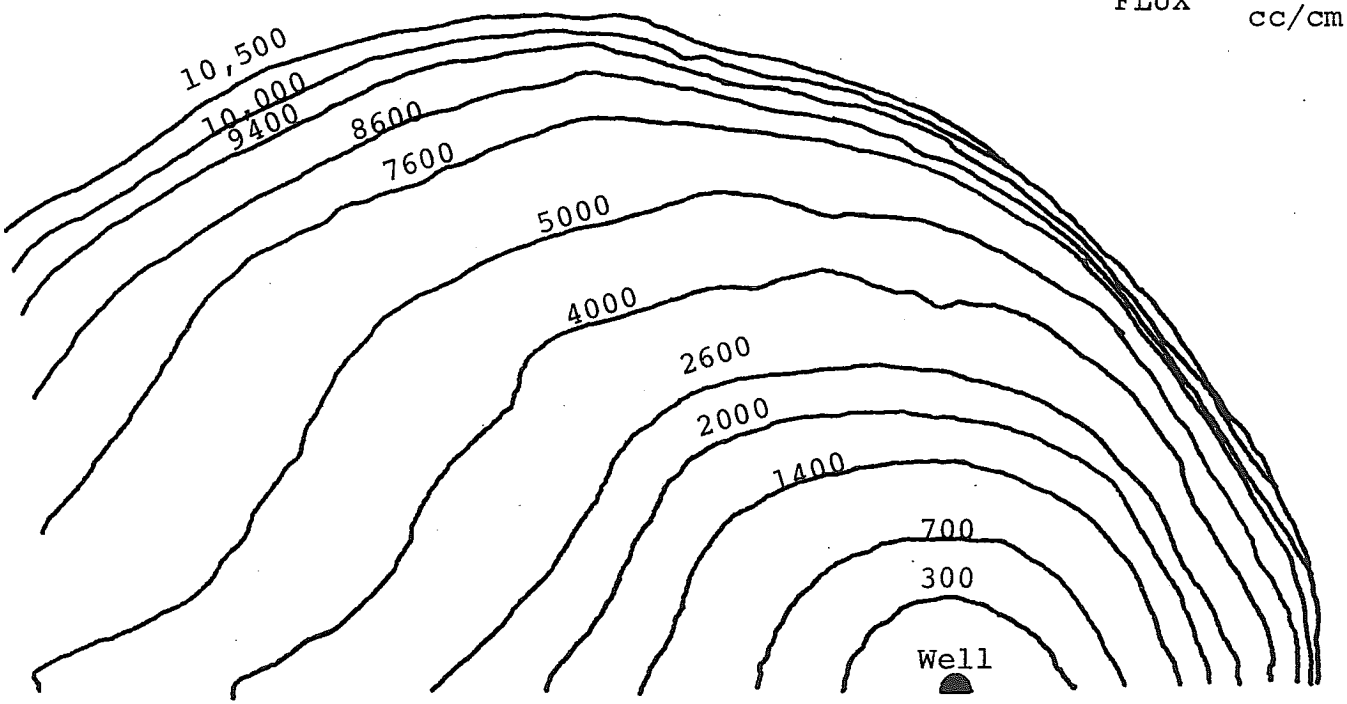

FIGURE 4.5 SELECTED FRONTAL POSITIONS FOR A HORIZONTAL RADIAL RUN WITH FLUX

comparison of Run 6 with Run 14 shows a beneficial effect of flux. Quantitative comparison is not warranted, however, because injection times are not the same in the two runs. Qualitatively, the effect of the flux is to retard the gravitational movement of the injected "bubble" in the direction of dip. A comparison of Runs 14 and 16 show strikingly the effect of reversing the direction of the flux.

It should be pointed out that there is an optimum rate of flux for an optimum recovery efficiency for each system being considered. A high flux rate for a small dip angle system would give a lower recovery efficiency compared to a no-flux case. As an example of such an optimum, refer to Table 4.4 and compare the first cycle recovery efficiency of Run 21 with those observed in Runs 19 and 20. All parameters were the same except for flux rate. Recoveries ranged from a low of 25 percent to a high of 50 percent.

As in the no-flux systems, the downdip front in some runs did not reach a point of equilibrium. For such a point to be achieved, the flux velocity vector must counterbalance the opposing vector due to gravity.

4.3 Results of Two Cycle Runs With Flux

Kumar reported that the recovery efficiency per cycle increases with total number of cycles even if the recovery efficiency for the first cycle is poor. His work was

TABLE 4.4

OBSERVED RECOVERY EFFICIENCY FOR TWO CYCLE RUNS IN RADIAL SYSTEMS WITH FLUX

Run No.	Dip Angle degrees	Density Difference gm/cc	Injection and Production Rates cc/sec	Flux Rate cc/cm^2-sec	Injection Time Per Cycle sec	Recovery Efficiency-% First Cycle	Second Cycle
19	15	0.22	0.0140	1.21×10^{-4}	25,500	47	55
20	15	0.22	0.0140	2.03×10^{-4}	25,500	25	24
21	15	0.22	0.0140	1.52×10^{-4}	25,500	50	57

conducted on a three dimensional horizontal radial flow mini-aquifer. In the present study, two cycle runs were conducted on a thin three dimensional dipping radial flow mini-aquifer with flux. In this more complex system, the recovery efficiency per cycle was also found to increase with the total number of cycles. This is true provided the rate of flux is relatively low as shown in Runs 19 and 21 of Table 4.4. If the flux rate is too high, then the recovery efficiency per cycle decreases with the total number of cycles as Run 20 indicates. Thus the normally expected benefits of multiple cycle operation may not always be obtained when dip and flux are present.

CHAPTER V

DESCRIPTION OF THE MATHEMATICAL MODEL

The mathematical model consists of two computer programs, AQUA I and PLOT I. Both programs are based on streamline tracking. AQUA I is a modified version of Painter's mathematical model, BUBBLE II. Laydown and mixed zone effects have been imposed on the model; the result was an improvement in the prediction of recovery efficiency.

PLOT I is a general program which tracks ten streamlines during the injection half cycle only. In addition, it estimates the point of equilibrium, that is the point at which a portion of the front moving against the flux stops. Such a prediction was performed only for Run 11 because it was the only run where a portion of the front was observed to stop advancing.

The forthcoming sections contain a comprehensive explanation of the computer programs and the phenomena upon which these programs are based.

5.1 Frontal Laydown

Painter's program, BUBBLE II, tracks 55 streamlines and only one of these streamlines, along the line of symmetry, is checked for breakthrough to predict recovery efficiency. It does not consider the effect of flux.

AQUA I tracks only two streamlines along the line of symmetry. Both of these streamlines are checked for breakthrough. It was assumed in Painter's study that piston-like displacement prevails in the thin model in both horizontal and dipping configuration during injection and production. Experimentally, however, this is not true. Even for a small density difference in a horizontal system, the frontal interface was observed to be inclined, not vertical, with respect to the surface of the mini-aquifer.

Therefore, modifications in Painter's computer model were necessary to bring model results into closer agreement with observation of the mini-aquifer. Two laydown procedures were developed in the computer program, AQUA I. The first implements the calculation of gravity segregation between two fluids at the end of the injection half cycle as calculated by Kumar. This segregation, being converted to radial geometry, is used to predict the inclination of the front in horizontal beds or beds with low dip angles. In the program, this laydown is represented by XR(NINT1), the length of the gravity segregation between two fluids at the end of the injection half cycle. This is the only position at which this correction is made.

In the second procedure, used in more steeply dipping systems, the front is placed horizontal at the end of the injection half cycle as shown in Figure 5.1. This would be the equilibrium position dictated by gravity. The

FIGURE 5.1 SCHEMATIC DIAGRAM OF PROCEDURE USED TO ESTIMATE MAXIMUM LAYDOWN IN A DIPPING SYSTEM

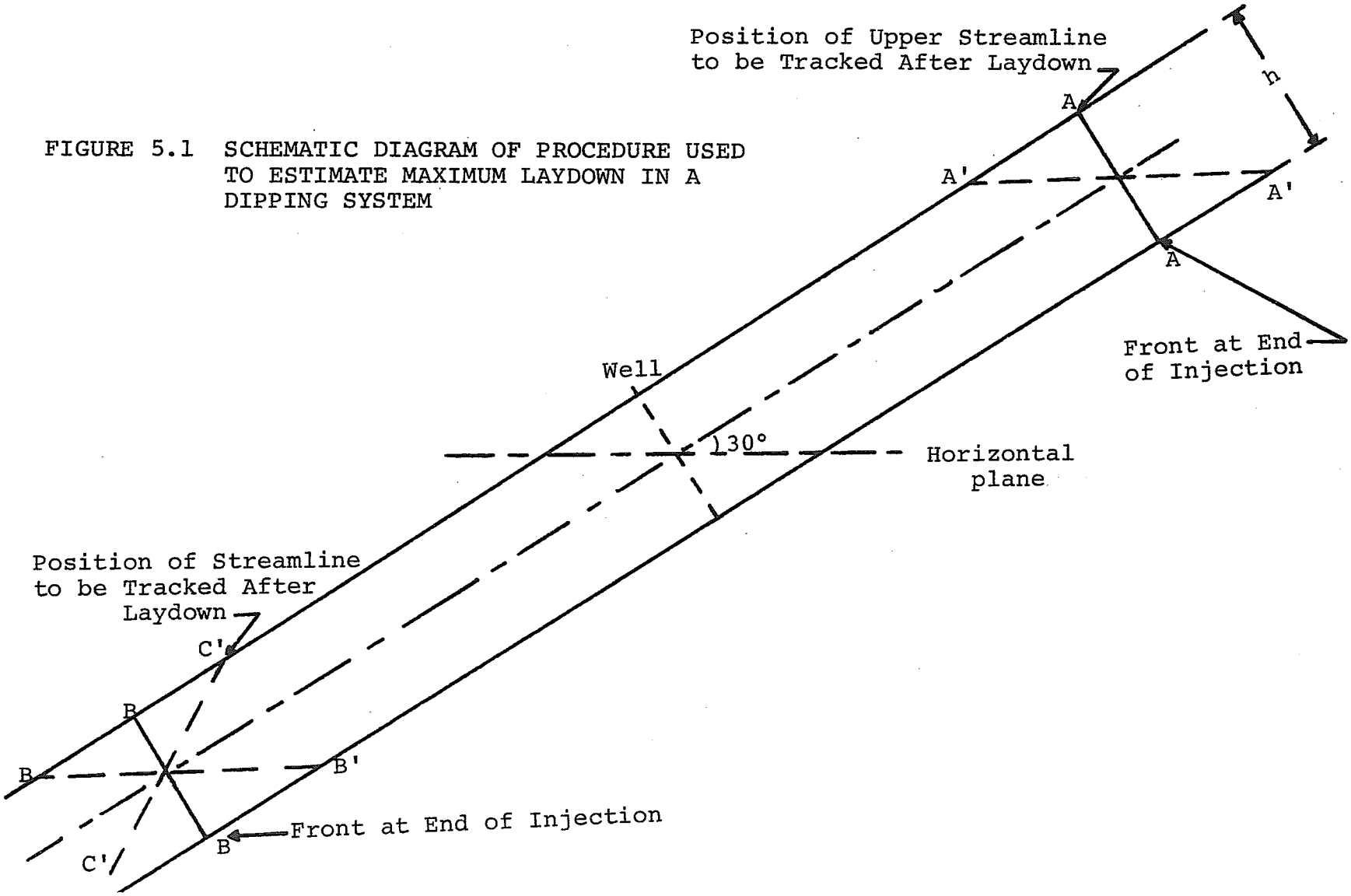

example shown assumes that the injected fluid is more dense than the reservoir fluid. The initial position of the front at the updip side is at A-A; after the laydown, the position is at A'-A'. At the downdip side, the front travels farther from the well than the updip side because of the gravity forces. The frontal position at the end of the injection half cycle is at B-B. After the laydown, the front is at C'-C'.

In the mathematical model, AQUA I, this horizontal laydown is represented by XCORR and evaluated as:

$$XCORR = \frac{1}{2} h \text{ X } TAN(90 - \alpha) \quad . \quad . \quad . \quad . \quad . \quad . \quad (5.1)$$

where

α = dip angle, degrees

h = thickness, cm.

In Figure 5.1, XCORR is the distance A A'.

Now, which laydown procedure is used depends on the dip angle. For horizontal beds, XR(NINT1) is used since XCORR is undefined. This is arbitrarily extended to beds with dip angles of 2 degrees or less. For larger angles, however, the program uses the procedure which gives the smaller laydown. It should be noted that at large angles, XR(NINT1) exceeds the equilibrium position, a situation which makes it unapplicable. After the laydown, the streamlines are tracked back to the well.

5.2 Mixed Zone Length

Diffusion and convective dispersion are the main phenomena responsible for mixed zone formation. In Painter's mathematical model, the effect of these phenomena was not included. For further improvements of the mathematical model, the effect of the mixed zone was incorporated. Kumar previously developed a computer program calculation procedure to estimate the recovery efficiency in a three dimensional radial system. This program included the calculation of the mixed zone length. This same calculation procedure is incorporated into the AQUA I program. In the program, this is referred to as "Mixed Zone Length Calculations." The following section shows the method of application.

5.3 Calculation of Recovery Efficiency

Computer program, AQUA I, is listed in Appendix C. It is restricted to two streamlines along the line of symmetry where, for the types of runs considered in this study, breakthrough occurs. If more streamlines are desired, a method for applying laydown and mixed zone to such streamlines must be developed.

The program can be subdivided into 4 parts. The first part develops the mixed zone lengths. The second develops the projection of the interface due to gravity segregation. The third corrects the projection of the interface to radial geometry. These three parts were

developed by Kumar for a three dimensional system and are being incorporated in this program.

The sole purpose of the fourth part is to calculate the recovery efficiency. The well is considered the origin and the starting circle is the wellbore radius RW. The "x" and "y" coordinates of each streamline are calculated. For the two streamlines being tracked, the initial "x" coordinates are RW and -RW. The "y" coordinates are zero.

The potential at any point (x, y) in one half of a radial system is given by,

$$\Phi(x, y) = - \frac{q\mu}{2\pi kh} \ln(x^2 + y^2) + \Phi_o \quad . \ . \ .(5.2)$$

where

q = actual injection or production rate in the half radial system, cc/sec

μ = viscosity of injected or produced fluid, cp

k = permeability, darcys

h = thickness, cm

Φ_o = potential at infinite radius, atmospheres

The potential gradient in the "x" and "y" directions is the derivative of Equation (5.2) with respect to "x" and "y" respectively given as:

$$\frac{\partial \Phi}{\partial x} = \Phi_x = - \frac{q\mu}{\pi kh} \left(\frac{x}{x^2 + y^2}\right) \ . \ . \ . \ . \ . \ .(5.3)$$

and

$$\frac{\partial \Phi}{\partial y} = \Phi_y = - \frac{q\mu}{\pi kh} \left(\frac{y}{x^2 + y^2}\right) \ . \ . \ . \ . \ . \ .(5.4)$$

The velocity components in the "x" and "y" directions are:

$$\vec{V}_x = -\frac{k}{\mu\phi}\Phi_x = -\frac{q}{\pi h\phi}\left(\frac{x}{x^2 + y^2}\right). \quad . \quad . \quad . \quad . \quad (5.5)$$

and

$$\vec{V}_y = -\frac{k}{\mu\phi}\Phi_y = -\frac{q}{\pi h\phi}\left(\frac{y}{x^2 + y^2}\right). \quad . \quad . \quad . \quad . \quad (5.6)$$

These gradients and velocities apply for either horizontal systems or dipping systems with no density difference. For dipping systems with density difference, the following velocity equation applies:

$$\vec{V}_x = \frac{q}{\pi h\phi}\left(\frac{x}{x^2 + y^2}\right) + 9.67 \times 10^{-4}\,\frac{k\Delta\rho\ \mathrm{Sin}\ \alpha}{\mu\phi}\left[\frac{2qt}{\pi\, r_e^{\,2}\, h\phi}\right]^{.17} \quad (2.10)$$

The second part on the right of the equality sign is the effect of the gravity forces. The time increment, DELT, for each step is calculated as

$$\mathrm{DELT} = \mathrm{DELX}\ /\sqrt{(\mathrm{VELX})^2} \quad . \quad . \quad . \quad . \quad . \quad . \quad . \quad (5.7)$$

where

DELX = constant distance increment, cm

VELX = velocity in the x direction, cm/sec, (a function of position and not constant)

The computer program starts the calculations by computing the initial values for the gradients and the velocities as described by Equation (5.3) through (5.6) and Equation (2.10) when applicable, using the initial "x" and "y" coordinates. Then DELT is computed using Equation (5.7).

Because of the potential gradients, the streamlines advance. In the "x" direction, the advancement is the velocity multiplied by the time increment. For dipping systems with density difference, however, the gravitational correction is added to VELX and then multiplied by the time increment, DELT. In the "y" direction, the advancement is VELY multiplied by DELT. For the two streamlines being tracked, this latter advancement is zero.

The first time increment is checked with the total injection time, a known value. If the increment is less, new values for the gradients, the velocities and the time increment are calculated using the most recent values for the "x" and "y" coordinates. These calculations utilize the same equations as in the first computational step. New "x" and "y" coordinates are computed as before.

Next, the cumulative injection time, the sum of the time increments is checked against the total injection time. If the cumulative is still less, more computational steps will be calculated. If both times are equal, the injection half cycle terminates. The front is then tilted by subtracting the appropriate value of XCORR from the prevailing "x" coordinates of the two streamlines.

To start the production half cycle, the sign of "q" is changed to negative. The streamlines will be tracked back toward the well in the same way they were tracked during the injection half cycle. Only the mixed zone lengths in the production half cycle are utilized. After

each of the first 4 computational steps, half the first mixed zone length in the production half cycle, R3(NINT1 + 1), where NINT1 is the number of intervals in the injection half cycle, will be subtracted from the prevailing absolute values of the "x" coordinates. And after each of these four steps, a test to check if either of the streamlines had broken through will be performed. If breakthrough has not occurred, streamline tracking continues. After each of the second four computational steps, half the second mixed zone length in the production half cycle, R3(NINT1 + 2) will be subtracted from the prevailing "x" coordinates. Then the breakthrough test will be performed. If breakthrough had not occurred, the tracking procedure continues. It should be pointed out that the mixed zone subtractions are used only in the test and do not affect the positions of the coordinates to be calculated.

Once one of the streamlines intersects the wellbore, recovery efficiency will be calculated as:

$$\text{REC. EFF.} = \frac{\text{Production Time Until Breakthrough}}{\text{Total Injection Time}}$$

This calculation procedure applies for both horizontal and dipping systems with unit mobility ratio.

In calculating the mixed zone lengths, the length of each interval, TILN, used in this program is 2.0 cms. DELX is 0.5 cms. The number "4" which was used in the previous paragraph is TILN/DELX. In AQUA I, it is

represented as NN. If either TILN or DELX is changed, NN must be changed.

For the runs incorporating flux, the potential gradient due to flux, represented as:

$$\Phi_{x\text{-FLUX}} = - \frac{q_{FLUX}\mu}{k \quad A} \quad \ldots\ldots\ldots (5.8)$$

where

$\Phi_{x\text{-FLUX}}$ = gradient in the x-direction due to flux, atmospheres/cm

q_{FLUX} = flux rate, cc/cm^2 - sec

A = total cross-sectional area, cm^2

is added to the potential gradient Φ_x due to injection. Except for this change, all computational steps are identical to the preceding.

5.4 Mathematical Description of Flow in Horizontal Runs

A computer program, PLOT I listed in Appendix D, was developed to track and plot streamlines for horizontal systems with and without flux. This program does not take into consideration interfacial tilt or mixed zone length.

The starting position is the circumference of a circle with a radius of 1.0 cm; the terminating point is 110.0 cm at either end. This program incorporates a constant starting time increment SDELT. If $(\Delta x^2 + \Delta y^2)^{1/2} > 0.5$ cm

where

Δx and Δy are distances travelled in the x and y directions respectively in one computational step,

the next time step increment is the same as the starting increment; if $(\Delta x^2 + \Delta y^2)^{1/2}$ is less than 0.5 cm, then the time increment is doubled. Potential gradients, velocities, and new "x" and "y" coordinates are calculated by the same equations used in the previous section. The potential gradient due to flux, C2, is included in the input data, and is incorporated in the calculations as in the preceding section.

Although the program does not plot frontal configurations, the output can be utilized to do so by connecting "x" and "y" coordinates of equal selected times of injection for all streamlines. Figure 5.2 compares such mechanically drawn fronts to those obtained experimentally for a run which is not listed in this study.

The equilibrium point, XSTOP, is the point at which the flux gradient, C2, equals the radial potential gradient in the "x" direction. For a full radial system, the radial potential gradient in rectangular coordinates is given by:

$$\frac{\partial \Phi}{\partial x} = - \frac{q\mu}{2\pi kh} \left(\frac{x}{x^2 + y^2}\right) = -C1\left(\frac{x}{x^2 + y^2}\right) \quad . \quad . \quad . \quad . (5.9)$$

However, the "y" coordinates of the equilibrium point along the line of symmetry is zero. Eliminating the "y" from Equation (5.9) and equating it to C2 yields,

$$C2 = -C1\left(\frac{x}{x^2}\right) = -C1\left(\frac{1}{XSTOP}\right) \quad . \quad . \quad . \quad . \quad . \quad . (5.10)$$

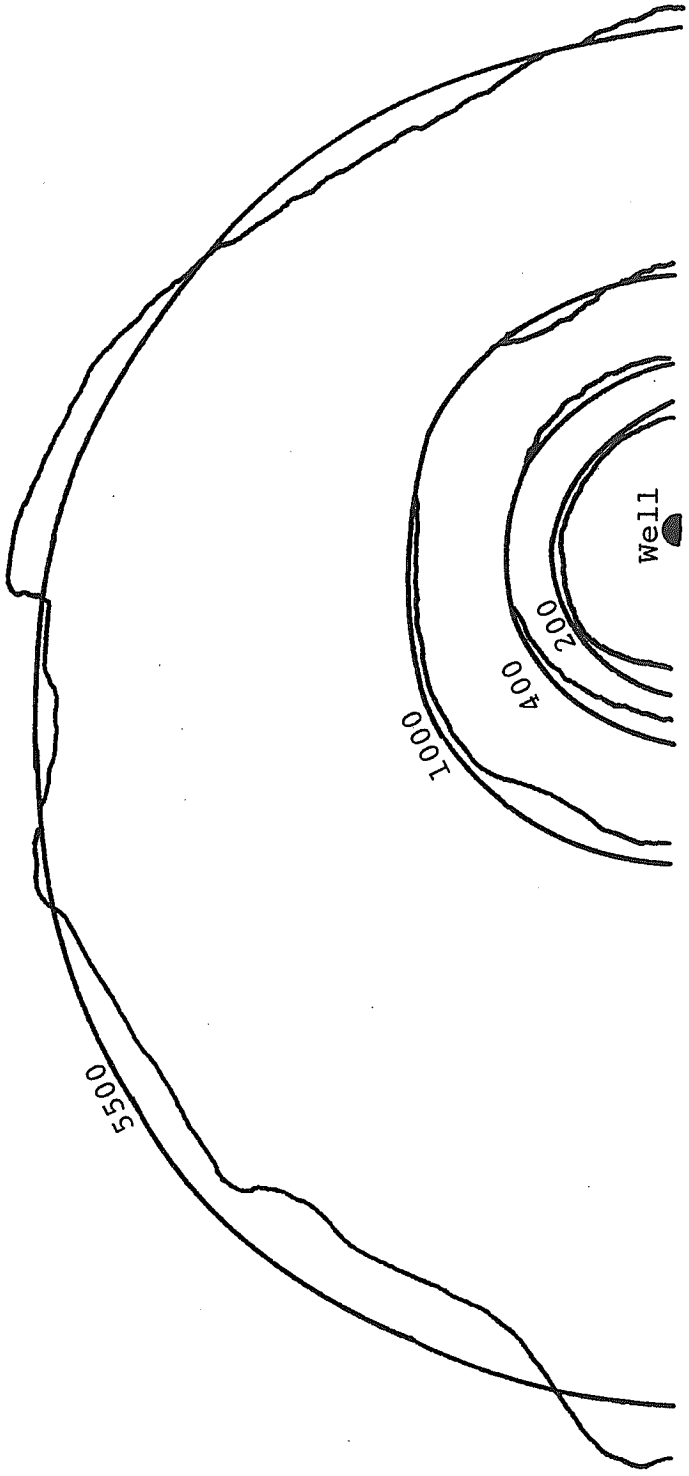

FIGURE 5.2 COMPARISON OF OBSERVED AND COMPUTED FRONTAL POSITIONS

and

$$XSTOP = -\frac{C1}{C2}.$$

Figure 5.3 is a streamline plot for Run 11. In it, ten image wells were incorporated to produce the effect of the no flow boundaries. XSTOP was calculated as 24.8 cm, represented by the shortest streamline to the right in Figure 5.3.

The graphical procedure consisted of superimposing the linear pressure distribution due to flux and the radial pressure distribution due to injection at the well. Figure 5.4 shows that $\frac{dp}{dr}$ becomes zero at a radius of approximately 25 cm from the wellbore. This is excellent agreement with the value computed by PLOT I. Figure 4.5 shows that the right front stopped advancing at an approximate distance of 18.4 cm as an observed value compared to 24.8 cm as computed by PLOT I. This difference in observed and predicted values could easily result from either inhomogeneity along the edge of the model or from the degree of accuracy with which the pressure drop due to flux alone was measured. Thus, these results are considered to be in reasonable agreement.

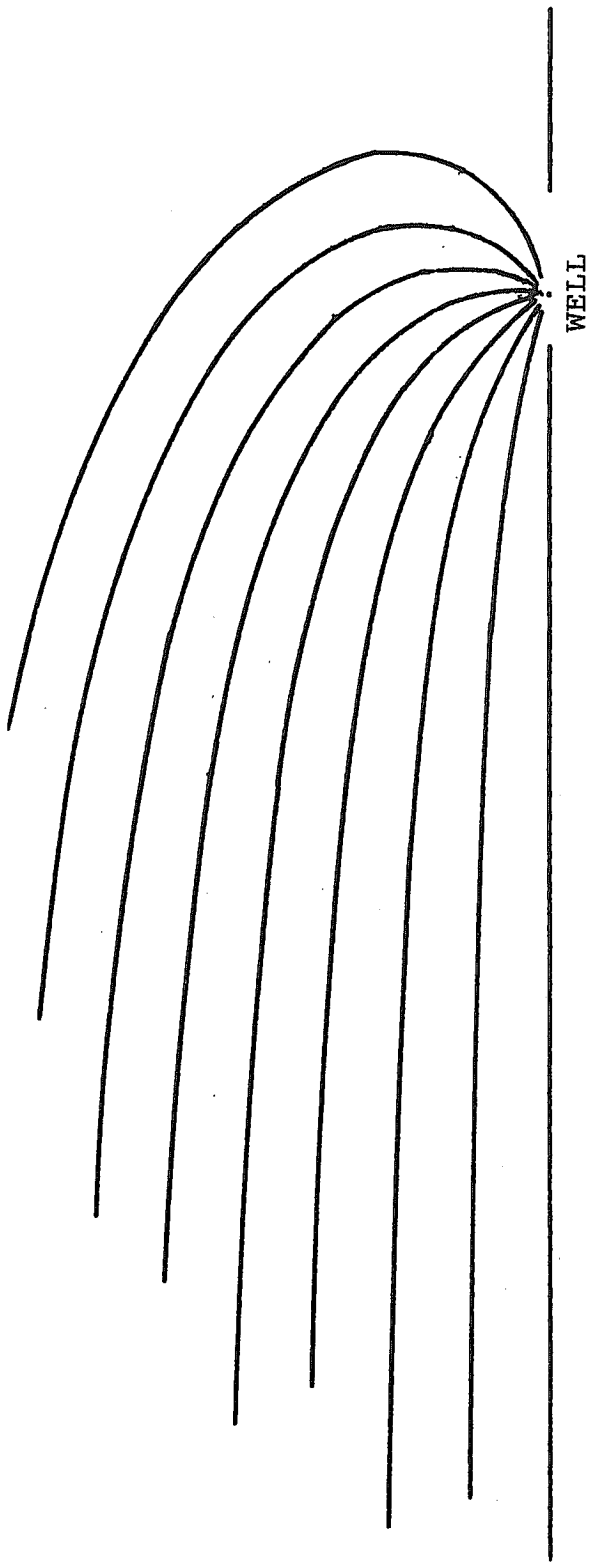

FIGURE 5.3 STREAMLINE PLOT FOR RUN 11

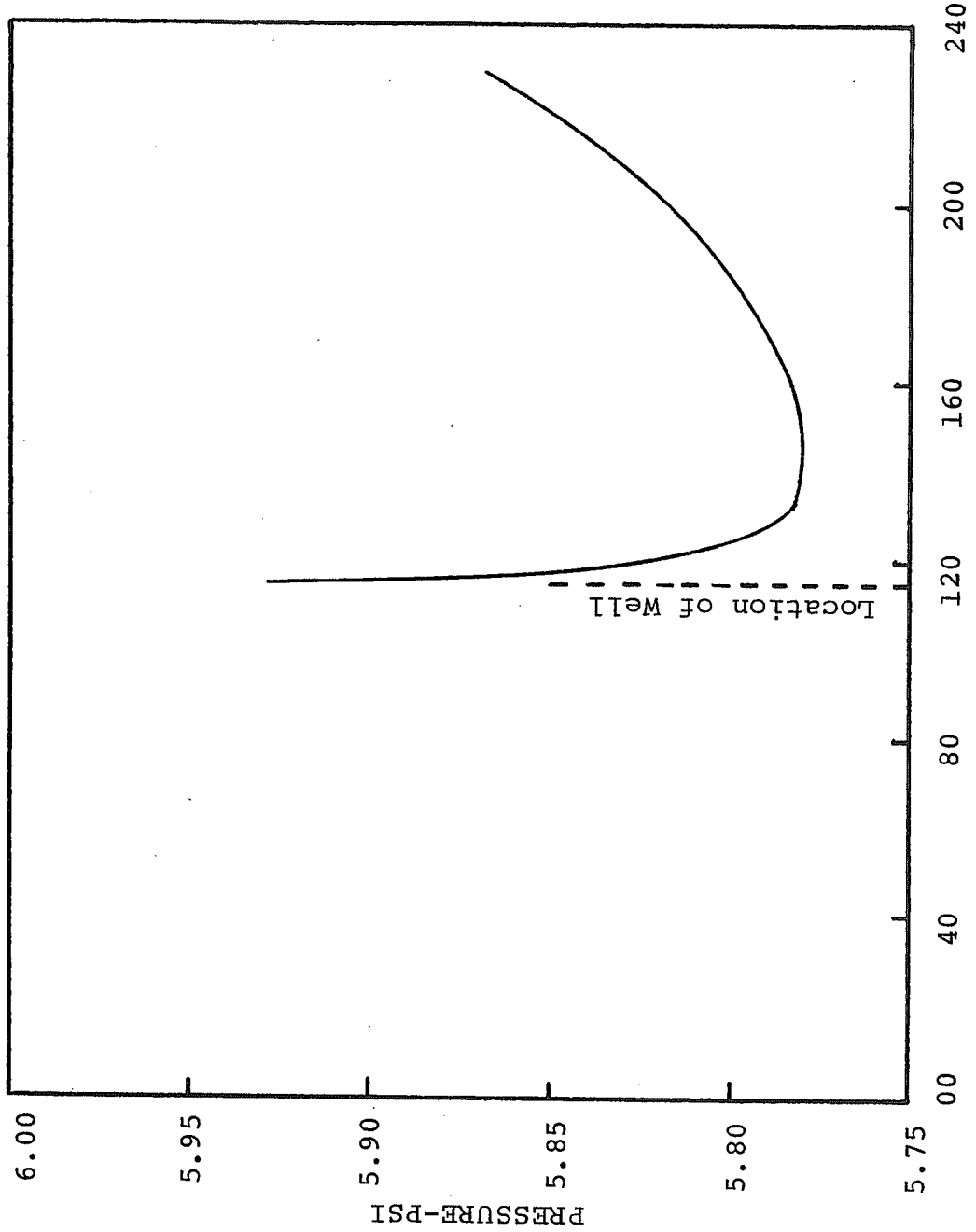

FIGURE 5.4 PRESSURE SUPERPOSITION

CHAPTER VI

COMPARISON OF CALCULATED AND OBSERVED RESULTS

Results of the mathematical model and observations of the mini-aquifer used in this study were in reasonable agreement. Although the mathematical model is restricted to cases with unit mobility ratio, it can accommodate all four types of runs investigated. Twenty one different runs were performed to obtain a wide variety of experimental results. For dipping systems with flux, in some cases the mathematical model, AQUA I, did not give an acceptable agreement with the observation.

6.1 Results of Horizontal Radial Runs Without Flux

The frontal advance of both horizontal and dipping radial runs computed by AQUA I was assumed to be piston-like during the injection half cycle. Two similar runs, Runs 1 and 2, were made in which no flux was present. Observed results are listed in Table 4.1. The mathematical model, AQUA I, predicted a recovery efficiency of 81% compared to 86% observed, which is satisfactory.

Kumar's mathematical model, which was developed for a three dimensional system and did not accommodate flux, was also used to predict the recovery efficiency for the horizontal no-flux case. Its prediction was 86% which is in excellent agreement with the observations. This

constitutes another validation of Kumar's program applicability to other physical models. It is not surprising that AQUA I, which incorporates parts of Kumar's program, gave a good agreement.

6.2 Results of Dipping Radial Runs With Flux

As might be expected, the present mathematical model improved the agreement between observed and predicted recovery efficiencies as compared to Painter's BUBBLE II program. Table 6.1 is a comparison of observed and predicted recovery efficiencies for a selected set of experiments by Painter. These runs were selected because an Oscillometer was used to predict the breakthrough, a reliable technique. The improved agreement is shown in Table 6.1.

Excellent agreement can be seen between observed values and predicted values by AQUA I in Table 6.2, a list of radial dipping runs without flux of the present study. The higher the density difference, the lower the recovery efficiency for the same dip angle, a situation shown by Runs 3 and 4.

Results shown in Table 6.1 indicate that the mathematical model, AQUA I, which implements Painter's exponent "n" (n = 0.17), is applicable to the circular isopotential model. In addition, Table 6.2 shows that the same program is applicable to the present semi-bounded physical model.

TABLE 6.1

COMPARISON OF OBSERVED AND PREDICTED RECOVERY EFFICIENCIES FROM PAINTER'S STUDY IN WHICH NO FLUX WAS PRESENT

Run No.	Dip Angle degrees	Density Difference gm/cc	Injection and Production Rates cc/sec	Injection Time sec.	Recovery Efficiency-% Painter's Observation	Painter's Prediction	Present Prediction
P-15	15.0	0.05	0.0033	26100	39	60	41
P-16	7.5	0.10	0.0486	6000	58	93	64
P-18	7.5	0.10	0.0182	17200	56	79	60
P-19	7.5	0.10	0.0512	13600	67	87	67
P-20	7.5	0.05	0.0668	5000	86	98	71

TABLE 6.2

COMPARISON OF OBSERVED AND PREDICTED RECOVERY EFFICIENCY FOR RADIAL DIPPING SYSTEMS WITHOUT FLUX

Run No.	Dip Angle degrees	Density Difference gm/cc	Injection and Production Rates cc/sec	Injection Time sec.	Recovery Efficiency %	
					Observed	Predicted
3	7.5	0.83	0.02645	11,400	22	29
4	7.5	0.05	0.0668	5,000	82	71
5	15.0	0.05	0.0278	13,150	73	69
6	15.0	0.21	0.0140	37,200	29	21
7	30.0	0.216	0.0668	7,200	46	49

Indications show that the dimensionless volumes, $\left[\frac{2qt}{\pi r_e^2 h\phi}\right]^{.17}$, should be based on distances to the no flow boundaries, whether these boundaries are caused by real or imaginary wells in a well field. This is an important result, for had it not been the case, the effect of gravity in dipping systems could not have been combined with the effect of flux.

6.3 Results of Horizontal and Dipping Runs With Flux

A comparison of observed and predicted recovery efficiencies for horizontal and dipping systems with flux is shown in Table 6.3. In most of the horizontal cases, AQUA I program predicts a recovery efficiency more than the observed. The agreement between observed and predicted recovery efficiencies was close in case of low recovery efficiency than in cases of high recovery efficiency. The poorest agreement is seen in runs with low flux rates. This short coming in the program results from the fact that the frontal laydown, which is very important in horizontal systems, is only applied at the end of the injection half cycle. This effect can be seen by comparing Runs 14 and 17. The front comes to an equilibrium position for high dip angles such as in Run 17.

It appears from Runs 18, 20 and 21 that in system of appreciable dip, the flux rate cannot be relied on to offset the high detrimental effect of dip. In Run 20, the

TABLE 6.3

COMPARISON OF OBSERVED AND PREDICTED RECOVERY EFFICIENCY FOR RADIAL SYSTEMS WITH FLUX*

Run No.	Dip Angle degrees	Density Difference gm/cc	Injection and Production Rates cc/sec	Flux Rate cc/cm^2-sec	Injection Time sec.	Recovery Efficiency-% Observed	Predicted
8	0.0	0.02	6.016	7.6×10^{-4}	7,200	23	18
9	0.0	0.02	6.016	4.3×10^{-4}	7,200	37	38
10	0.0	0.02	6.016	2.2×10^{-4}	7,200	59	60
11	0.0	0.02	3.676	6.1×10^{-4}	10,500	17	18
12	0.0	0.017	4.010	0.84×10^{-4}	7,200	50	69
13	0.0	0.021	4.010	0.25×10^{-4}	7,200	80	76
14	15.0	0.210	0.840	0.84×10^{-4}	15,000	52	57
15	15.0	0.22	0.840	0.84×10^{-4}	25,000	46	47
*16	15.0	0.23	0.840	0.84×10^{-4}	15,000	14	19
19	15.0	0.22	0.840	1.21×10^{-4}	25,500	47	65
20	15.0	0.22	0.840	2.03×10^{-4}	25,500	25	40
21	15.0	0.22	0.840	1.52×10^{-4}	25,500	50	98
17	30.0	0.215	0.840	0.84×10^{-4}	15,200	20	28
18	30.0	0.21	0.840	1.9×10^{-4}	15,000	27	57

* Flux direction is updip in all runs except Run 16 in which it is downdip.

flux was so high that the lower streamline broke through fast. Thus, an optimum probably exists between the conditions of Runs 20 and 21. For high dip angles, the optimum recovery efficiency may be low. Comparing Runs 15 and 21 in Table 6.3 shows an improvement of 4% in observed recovery efficiency by almost doubling the flux rate.

CHAPTER VII

CONCLUSIONS AND RECOMMENDATIONS

7.1 Conclusions

1. The alteration in the outer boundary of the mini-aquifer from a semicircular isopotential to a semi-bounded system produced only a minor effect on the configuration of the injected "bubble." This is valid provided the "bubble" does not advance more than 30% of the distance from the well to the closed boundary. For larger injected volumes, a pronounced flattening of the "bubble" occurred on the side toward the closed boundary.

2. In spite of small changes in frontal configuration, the effect of the altered outer boundary on the observed recovery efficiency was minor.

3. The mathematical approach employed by Painter appears to also be valid for a bounded system such as employed in the present study provided the injected fluid does not closely approach the closed boundary.

4. Although the mini-aquifer is thin, it must be treated mathematically as a three dimensional system since under most conditions the effect of frontal inclination is significant.

5. The mathematical model presented by Kumar appears to adequately predict the behavior of the present (bounded) mini-aquifer when neither dip nor flux is present. This

constitutes a validation of Kumar's mathematical model in a mini-aquifer with characteristics that are appreciably different from that which he employed.

6. Flux in horizontal systems decreases the recovery efficiency, regardless of the density difference between the two fluids or the injection and production rates.

7. Flux acting in a direction which opposes gravitational migration of an injected "bubble" in dipping systems increases the recovery efficiency for relatively low flux rates. Other parameters being held constant, an optimum recovery efficiency which is dependent on flux rate would exist. This optimum may be at relatively low values of recovery efficiency in the case of high density differences, low injection rates, and high dip angles. In a practical situation, of course, the flux rate existing in the aquifer is fixed and not subject to alteration.

8. The mathematical model presented in this study appears to adequately predict recovery efficiency in horizontal systems, of the type studied, both with and without flux, and in dipping systems without flux. In dipping systems with flux, however, the prediction in some instances was poor.

7.2 Recommendations

1. The mathematical model, PLOT I, presented should be extended to give a description of the entire frontal configuration in horizontal and dipping systems with flux.

The extended model should be checked against the experimental data obtained in the present study.

2. The present mathematical treatment should be extended to include formation stratification.

3. A mini-aquifer which incorporates formation stratification, should be constructed and studied.

NOMENCLATURE

A = cross-sectional area, cm^2

C = concentration, volume fraction

D = diffusion coefficient, cm^2/sec

$$\text{erf}(\xi) = \frac{2}{\sqrt{\pi}} \int_0^{\xi} e^{-w^2}\, dw$$

g = gravitational acceleration $\equiv$ 980 cm/sec^2

g_c = unit conversion constant

h = thickness, cm

k = permeability, darcys

L = total length, cm

ln = natural logarithm

n = exponent

P = pressure, atm

q = flow rate, cc/sec

q_{FLUX} = flow rate due to flux, cc/cm^2 - sec

Q = $q/2\pi h\phi$, cm^2/sec

r = radius, cm

t = time, sec

S = density gradient, gm/cm^4

T_d = dimensionless time $\equiv \dfrac{q_i \gamma}{2A\phi L}\, t$

V = velocity, cm/sec

X = distance in the "x" direction, cm

y = distance in the "y" direction, cm

$\left[\frac{q_i t}{AL\phi}\right]$ = dimensionless pore volumes injected

XCORR = correction for laydown, cm

B = Volume formation factor, bbl/STB

Greek

μ = viscosity, cp

ρ = density, gm/cc

α and σ = longitudinal coefficient of convective dispersion, cm

α = dip angle (when used with Sin or Tan), degrees

γ = gross system parameter $\equiv 3.89 \times 10^{-3} \frac{k\Delta\rho \text{ Sin } \alpha}{\mu q_i}$

ϕ = porosity, fraction

ϕ_D = displacable porosity, fraction

Φ = potential, atm

Subscripts

d = down-dip

e = external

g = gravity

i = injection

u = up-dip

w = wellbore

x = direction coinciding with dip

y = direction perpendicular to dip

SELECTED REFERENCES

1. Kimbler, O. K., Kazmann, R. G., Whitehead, W. R., "Saline Aquifers-Future Storage Reservoirs For Fresh Water?" To be presented at International Symposium on Underground Waste Management and Artificial Recharge, New Orleans, Sept. 1973.

2. Esmail, O. J., "Investigation of the Technical Feasibility of Storing Fresh Water in Saline Aquifers", M.S. Thesis, Louisiana State U., Baton Rouge (Aug., 1966).

3. Kumar, A., and Kimbler, O. K., "Dispersion and Gravity Segregation of Miscible Fluids in Porous Media for Stratified Radial Flow Systems", Journal of Water Resources Research (1970) Vol. 6, No. 6, 1699.

4. Painter, T. R., "Unequal Density Miscible Displacements in Thin Homogeneous Tilted Beds", M.S. Thesis, Louisiana State U., Baton Rouge (Dec. 1971).

5. Raimondi, P., Gardner, G. H., and Petrick, C. B., "Effect of Pore Structure and Molecular Diffusion on the Mixing of Miscible Fluids Flowing in a Porous Media." Preprint 43, AICHE-SPE Joint Symposium on Fundamental Concepts of Miscible Displacement, Part II, San Francisco (Dec. 6-9, 1959).

6. Kumar, A., "Dispersion and Gravity Segregation of Miscible Fluids in Porous Media For Stratified Radial Flow Systems", M.S. Thesis, Louisiana State U., Baton Rouge (Jan. 1968).

7. Gardner, G. H. F., Downie, J. and Kendal, H. A., "Gravity Segregation of Miscible Fluids in Linear Models", Trans. AIME (1962) Vol. 225, 95.

8. Esmail, O. J., and Kimbler, O. K., "Investigation of the Technical Feasibility of Storing Fresh Water in Saline Aquifers", Journal of Water Resources Research (1967) Vol. 3, No. 3, 688.

APPENDIX A

PRESSURE SUPERPOSITION

The following calculations are based on data obtain from Run 11.

Data:

$q = 3.6765$ cc/min

$h = 1.0$ cm

$k = 5.09$ darcys

$\mu = 1.06$ cp

$B = 1.0$ BBL/STB

Pressure at the end where flux is introduced = 3.10 psi (gauge reading).
Pressure at the opposite end = 2.717 psi - measured as the pressure exerted by the column of fluid from the reservoir to the isopotential.

The flow rate equation for a radial system is

$$q_{sc} = \frac{7.08\ kh\ P_e - P_w}{\mu B\ \ln(\frac{r_e}{r_w})} \quad \ldots\ldots\ldots (A.1)$$

Convert the above data to field units, where

$q = 1.9979$ BBL/day

$h = 3.2808 \times 10^{-2}$ ft.

Substitute in Equation (A.1) and solve for $P_e - P_w$, Equation (A.1) becomes:

$$P_e - P_w = 0.0527\ \ln(\frac{r_e}{r_w}) \quad \ldots\ldots\ldots (A.2)$$

where

$P_e - P_w$ = pressure drop as a function of $\ln(\frac{r_e}{r_w})$, psi

r_e = outer boundary = 115 cm

For the linear system represented by the flux flow, the flow rate equation is

$$q = 1.127 \frac{kA(P_e-P_w)}{\mu L} \quad \ldots\ldots\ldots (A.3)$$

where

A = total cross sectional area = 0.1184 ft^2

L = total length of model = 7.5458 ft

k = permeability = 5.09 darcys

Solving for P_e-P_w, Equation (A.3) yields

$$P_e-P_w = 0.2062\ L \quad \ldots\ldots\ldots (A.4)$$

as a linear function with slope of 0.2062.

Table A.1 lists the pressures that result from linear and radial flow at varying values of r_w. The starting point is the wellbore radius and the ending point is the isopotential where the flux is introduced - a radius of 115 cm. The linear pressure in column 4 was read directly from Figure A.1. ΔP in column 2 had been calculated using Equation (A.2). To it, the pressure at the isopotential, 2.717 psi, was added giving the radial pressure distribution as listed in column 3 and plotted in Figure A.1. The sum of the linear and the radial pressure distributions gives the superimposed pressures in column 5. The

TABLE A.1

SUPERPOSITION OF PRESSURES
IN A HORIZONTAL SYSTEM WITH FLUX

Well Radius RW cm.	ΔP psi	Radial Pressure (ΔP + 2.71) psi	Linear Pressure psi	Super-imposed Pressure psi
0.625	0.2748	2.9925	2.935	5.9275
5.0	0.1659	2.8836	2.940	5.8236
10.0	0.1287	2.8464	2.950	5.7964
15.0	0.1073	2.8250	2.960	5.7850
20.0	0.0921	2.8098	2.970	5.7798
25.0	0.0804	2.7981	2.980	5.7781
27.0	0.0763	2.7940	2.985	5.7790
30.0	0.0708	2.7885	2.990	5.7792
35.0	0.0626	2.7803	3.000	5.7803
40.0	0.0556	2.7733	3.010	5.7813
45.0	0.0494	2.7671	3.015	5.7821
50.0	0.0438	2.7615	3.025	5.7865
75.0	0.0225	2.7402	3.075	5.8752
100.0	0.0073	2.7250	3.115	5.8400
115.0	0.0000	2.7177	3.15	5.8677

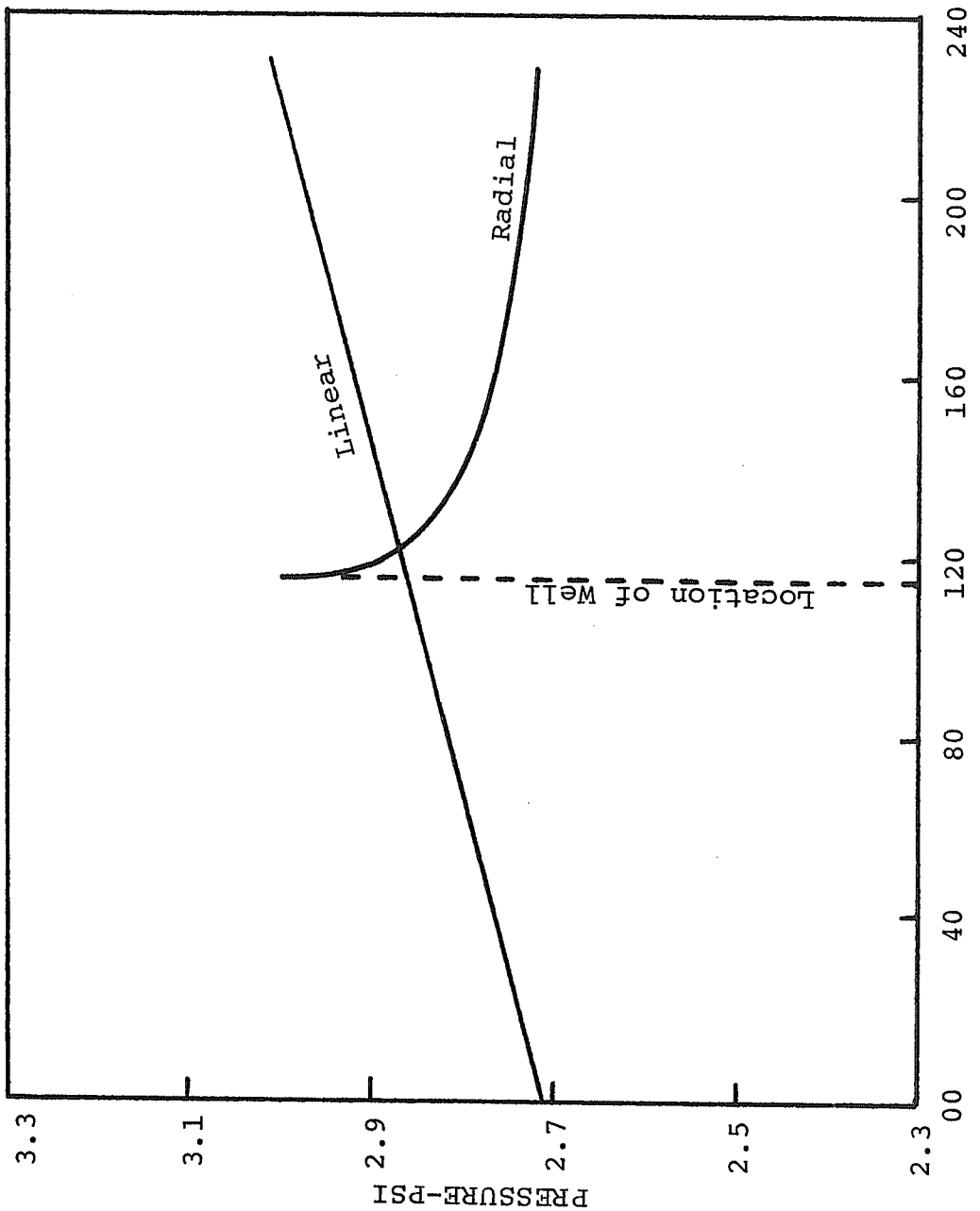

FIGURE A-1 LINEAR AND RADIAL PRESSURE DISTRIBUTIONS

plot is shown in Figure 5.4 where superimposed pressures are plotted against linear distance. This superposition was used in Chapter V to predict the point of equilibrium.

APPENDIX B

EXPERIMENTAL DATA

TABLE B-1

LIST OF ALL RUNS PERFORMED IN THIS STUDY

Run No.	Dip Angle degrees	Density Difference gm/cc	Injection and Production Rates cc/sec	Flux Rate cc/cm^2-sec	Injection Time sec.	Observed Recovery Efficiency %	Predicted Recovery Efficiency %
1	0.0	0.02	0.1002	0.0	7,200	86	81
2	0.0	0.02	0.1002	0.0	7,200	87	81
3	7.5	0.83	0.0264	0.0	11,400	22	29
4	7.5	0.05	0.0668	0.0	5,000	82	71
5	15.0	0.05	0.0278	0.0	13,150	73	69
6	15.0	0.21	0.0140	0.0	37,200	29	21
7	30.0	0.216	0.0668	0.0	7,200	46	49
8	0.0	0.02	0.1002	7.6×10^{-4}	7,200	23	18
9	0.0	0.02	0.1002	4.3×10^{-4}	7,200	37	38
10	0.0	0.02	0.1002	2.2×10^{-4}	7,200	59	60
11	0.0	0.02	0.0612	6.1×10^{-4}	10,500	17	18
12	0.0	0.017	0.0668	0.84×10^{-4}	7,200	50	60
13	0.0	0.021	0.0668	0.25×10^{-4}	7,200	80	76
14	15.0	0.210	0.0140	0.84×10^{-4}	15,000	52	57
15	15.0	0.220	0.0140	0.84×10^{-4}	25,000	46	47
16	15.0	0.230	0.0140	0.84×10^{-4}	15,000	14	19
17	30.0	0.215	0.0140	0.84×10^{-4}	15,200	20	28
18	30.0	0.21	0.0140	1.9×10^{-4}	15,000	27	57
19	15.0	0.22	0.0140	1.21×10^{-4}	25,500	47	65
20	15.0	0.22	0.0140	2.03×10^{-4}	25,500	25	40
21	15.0	0.22	0.0140	1.52×10^{-4}	25,500	50	98

RUN NUMBER 1

Scale: Inches

0 1 2 3 4

INJECTION _____

PRODUCTION ----------

$\alpha = 0.0°$

$\Delta\rho = 0.02$ gm/cc

$q = 0.1002$ cc/sec

(NO FLUX)

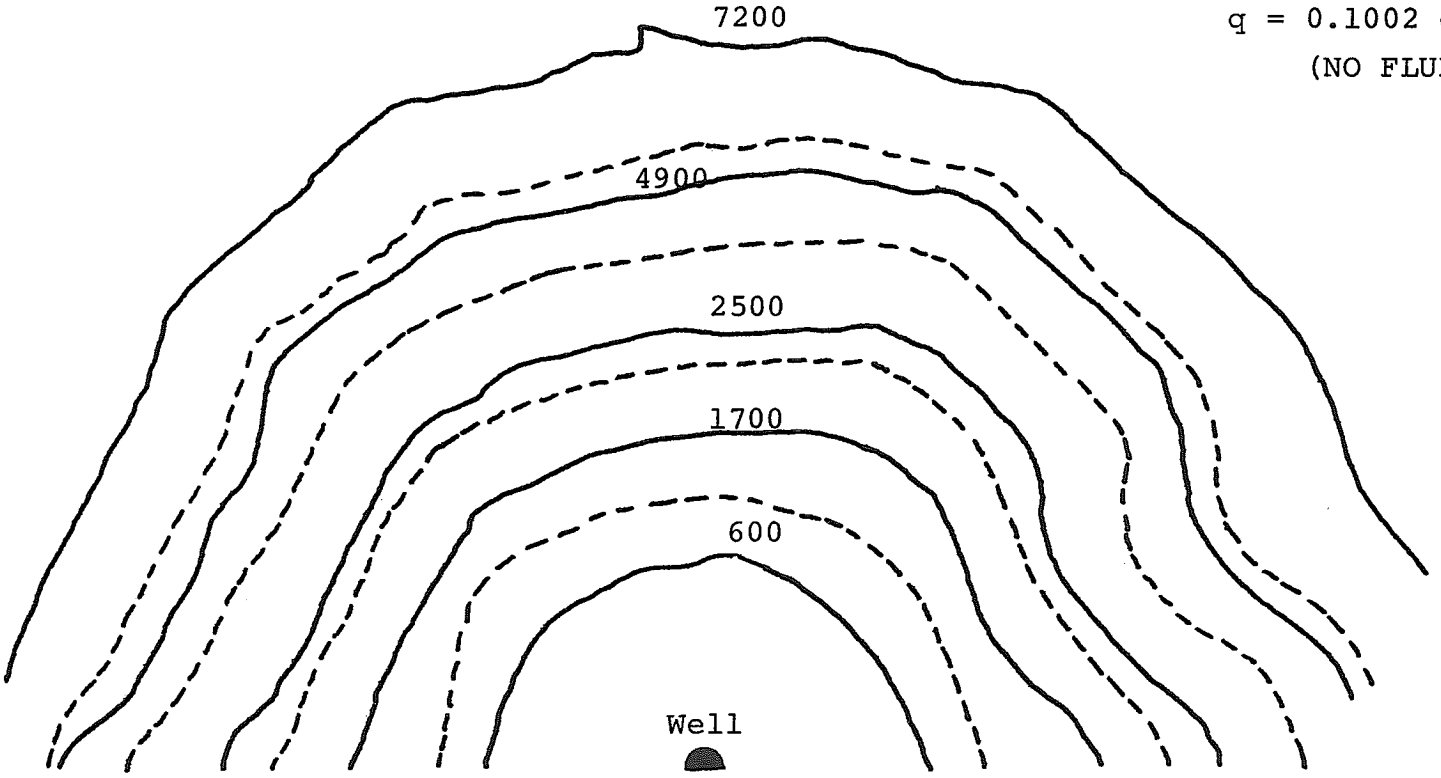

RUN NUMBER 2

Scale: Inches

0 1 2 3 4

INJECTION _____

PRODUCTION ----------

$\alpha = 0.0°$

$\Delta\rho = 0.02$ gm/cc

$q = 0.1002$ cc/sec

(NO FLUX)

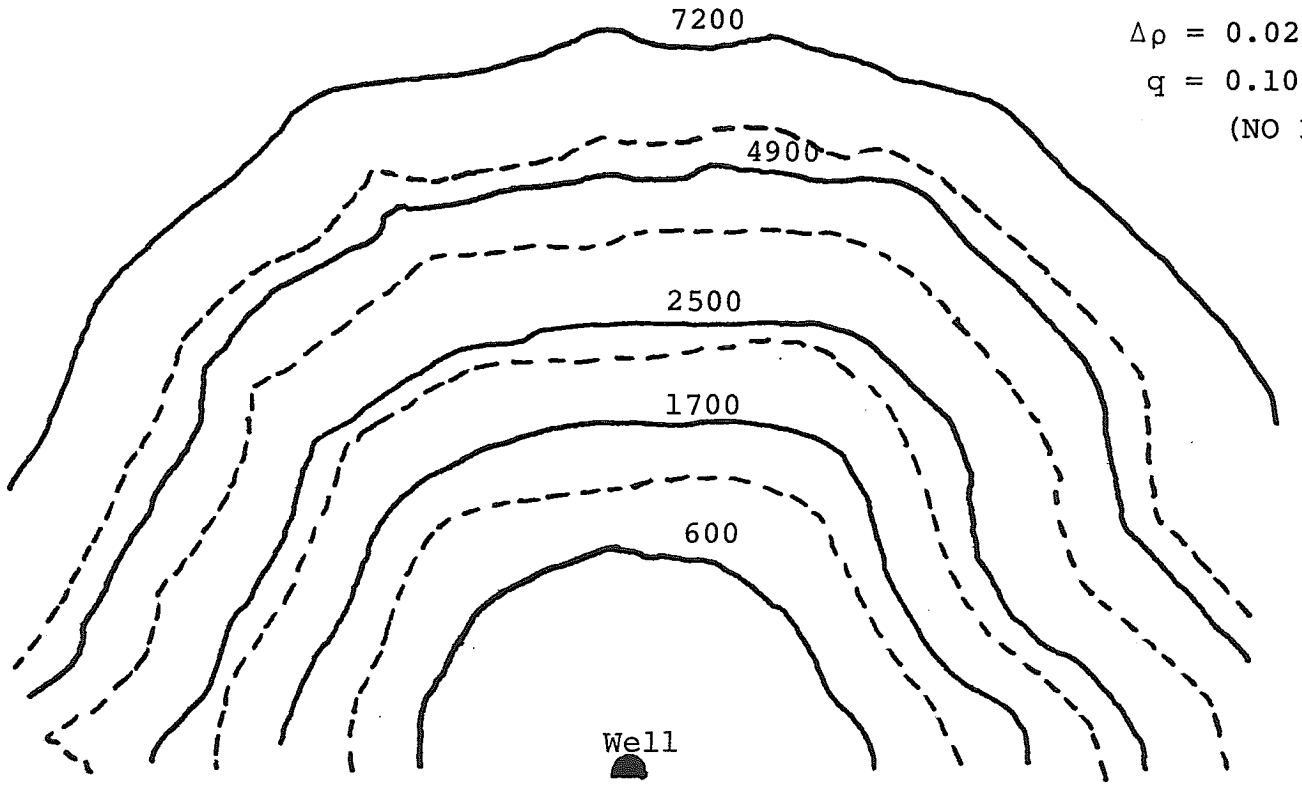

RUN NUMBER 3

Scale: Inches

0 1 2 3 4

INJECTION _____

PRODUCTION ----------

α = 7.5°

$\Delta\rho$ = 0.83 gm/cc

q = 0.0264 cc/sec

(NO FLUX)

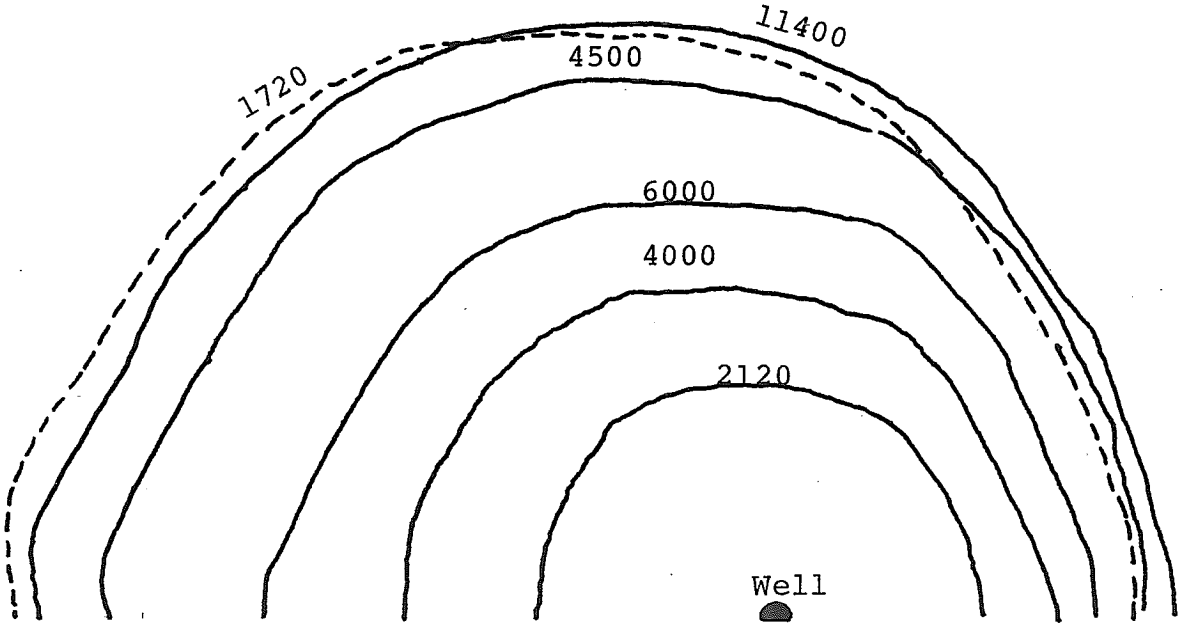

RUN NUMBER 4

Scale: Inches

0 1 2 3 4

INJECTION _____

PRODUCTION ----------

$\alpha = 7.5°$

$\Delta\rho = 0.05$ gm/cc

$q = 0.0668$ cc/sec

(NO FLUX)

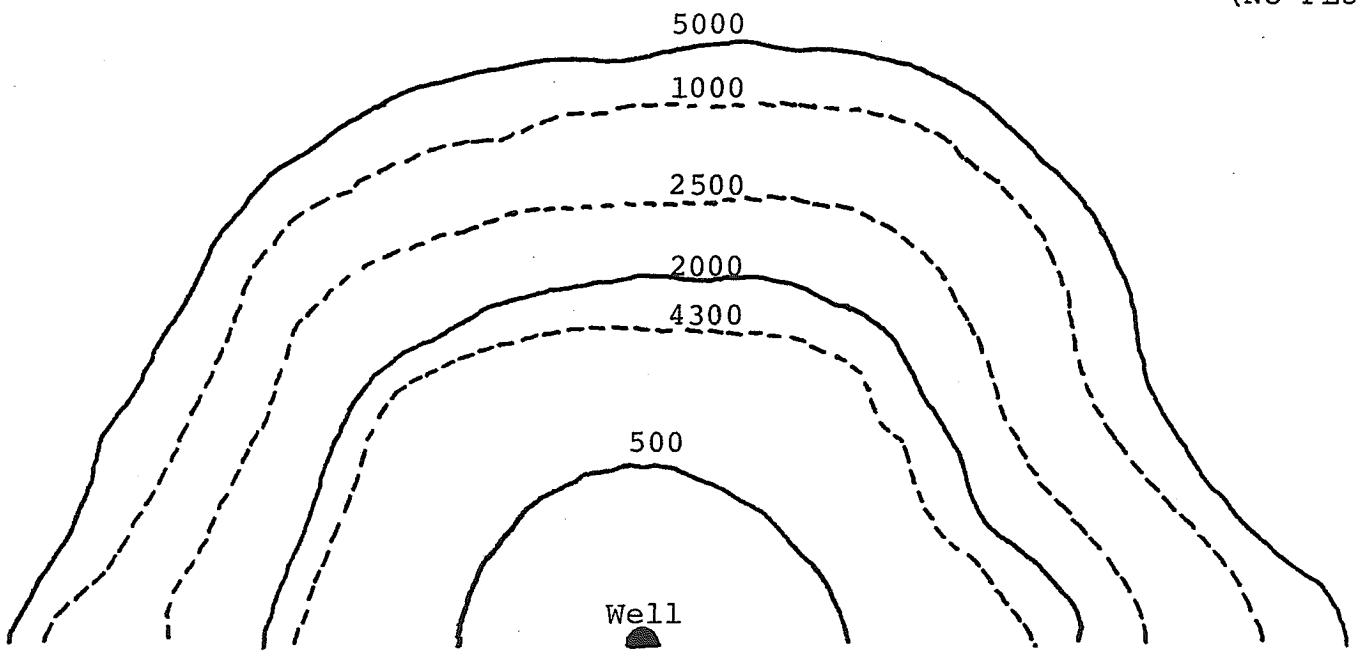

RUN NUMBER 5

Scale: Inches

0 1 2 3 4

INJECTION _____

PRODUCTION ----------

α = 15.0°

$\Delta\rho$ = 0.05 gm/cc

q = 0.0278 cc/sec

(NO FLUX)

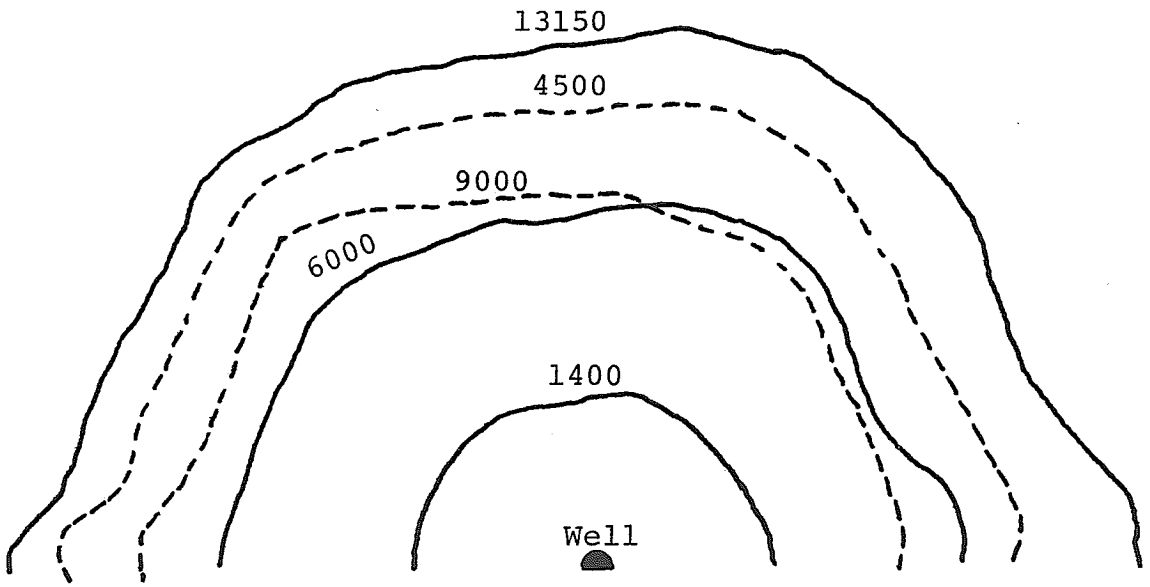

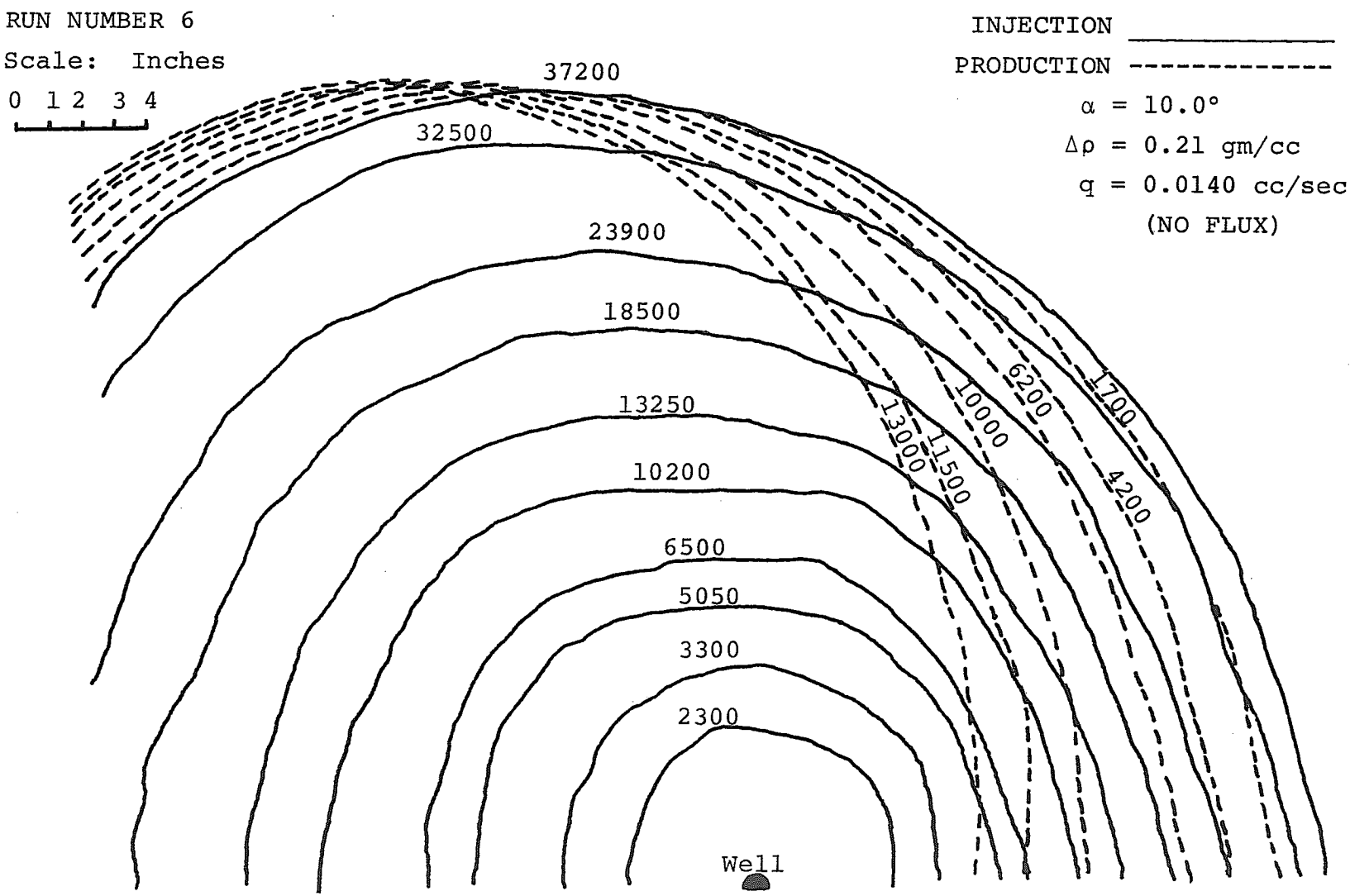
RUN NUMBER 6
Scale: Inches
0 1 2 3 4
INJECTION
PRODUCTION
α = 10.0°
Δρ = 0.21 gm/cc
q = 0.0140 cc/sec
(NO FLUX)
37200
32500
23900
18500
13250
10200
6500
5050
3300
2300
1700
4200
6200
10000
11500
13000
Well

RUN NUMBER 7

Scale: Inches

0 1 2 3 4

INJECTION _____

PRODUCTION ----------

α = 30.0°

$\Delta\rho$ = 0.216 gm/cc

q = 0.0668 cc/sec

(NO FLUX)

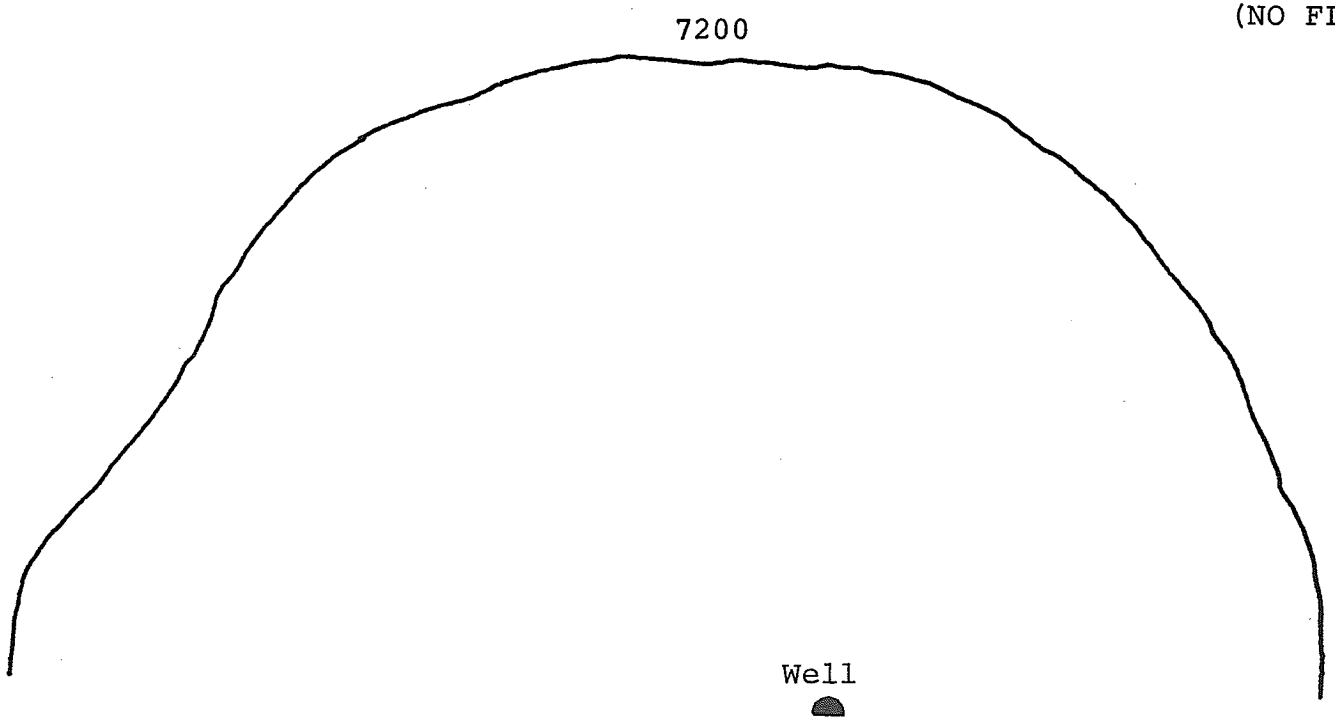

RUN NUMBER 8

Scale: Inches

0 1 2 3 4

INJECTION _____

PRODUCTION ----------

$\alpha = 0.0°$

$\Delta\rho = 0.02$ gm/cc

$q = 0.1002$ cc/sec

$q_{FLUX} = 7.6 \times 10^{-4}$ cc/cm^2 - sec

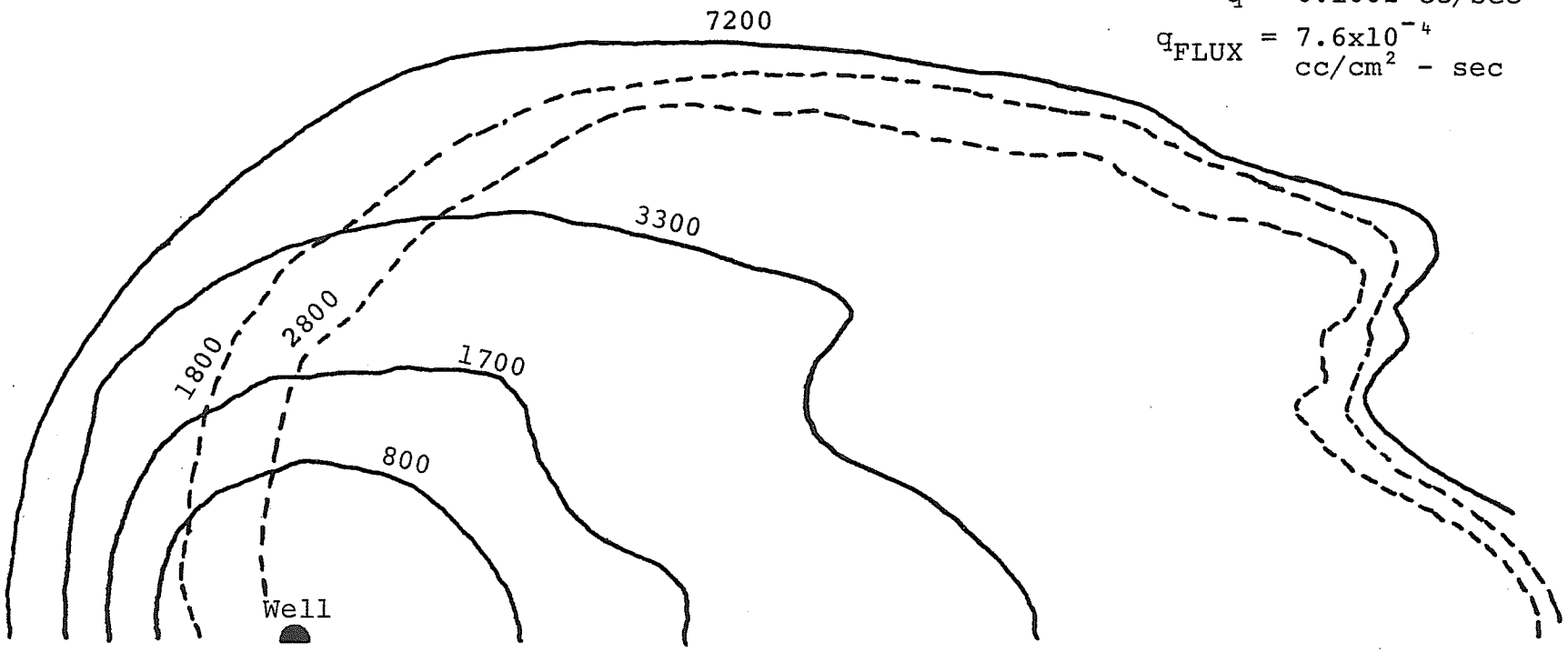

RUN NUMBER 9

Scale: Inches

0 1 2 3 4

INJECTION _____

PRODUCTION ----------

$\alpha = 0.0°$

$\Delta\rho = 0.02$ gm/cc

$q = 0.1002$ cc/sec

$q_{FLUX} = \frac{4.3 \times 10^{-4}}{cc/cm^2 - sec}$

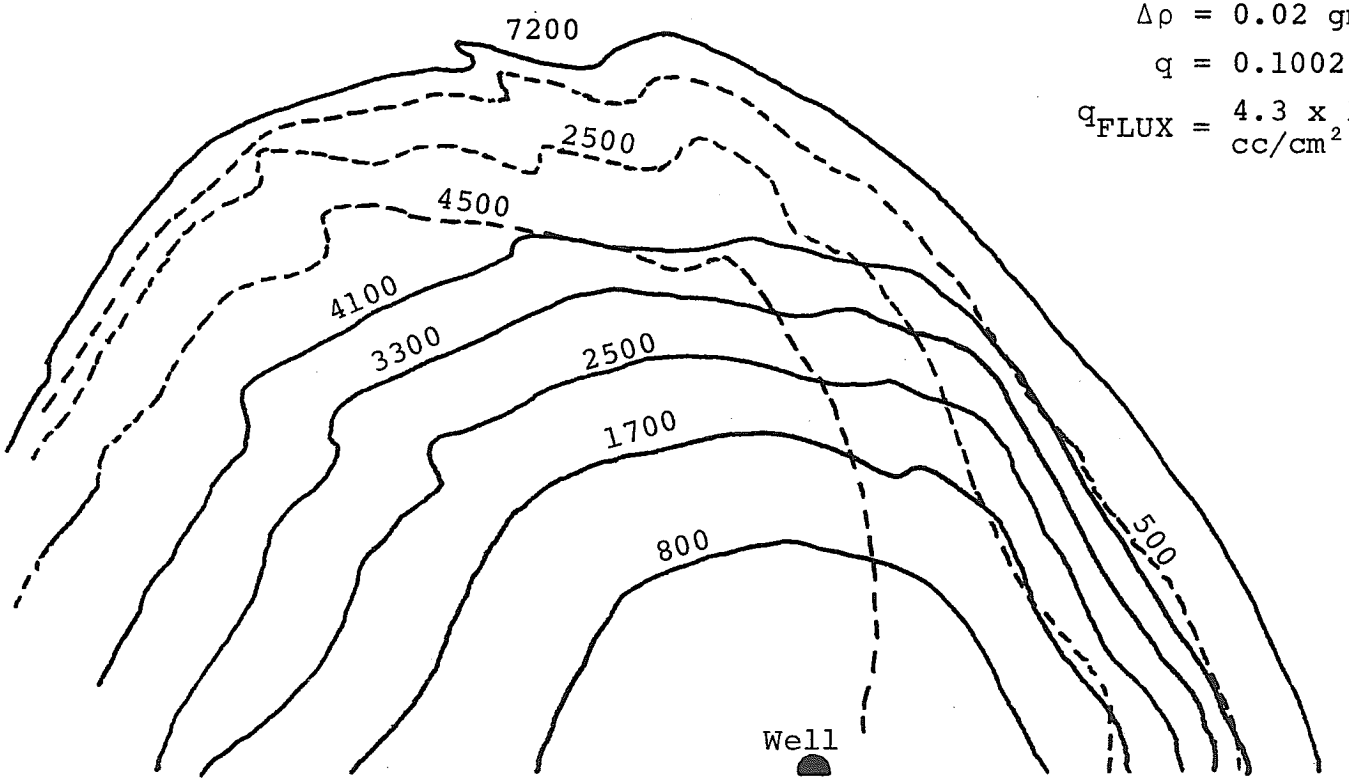

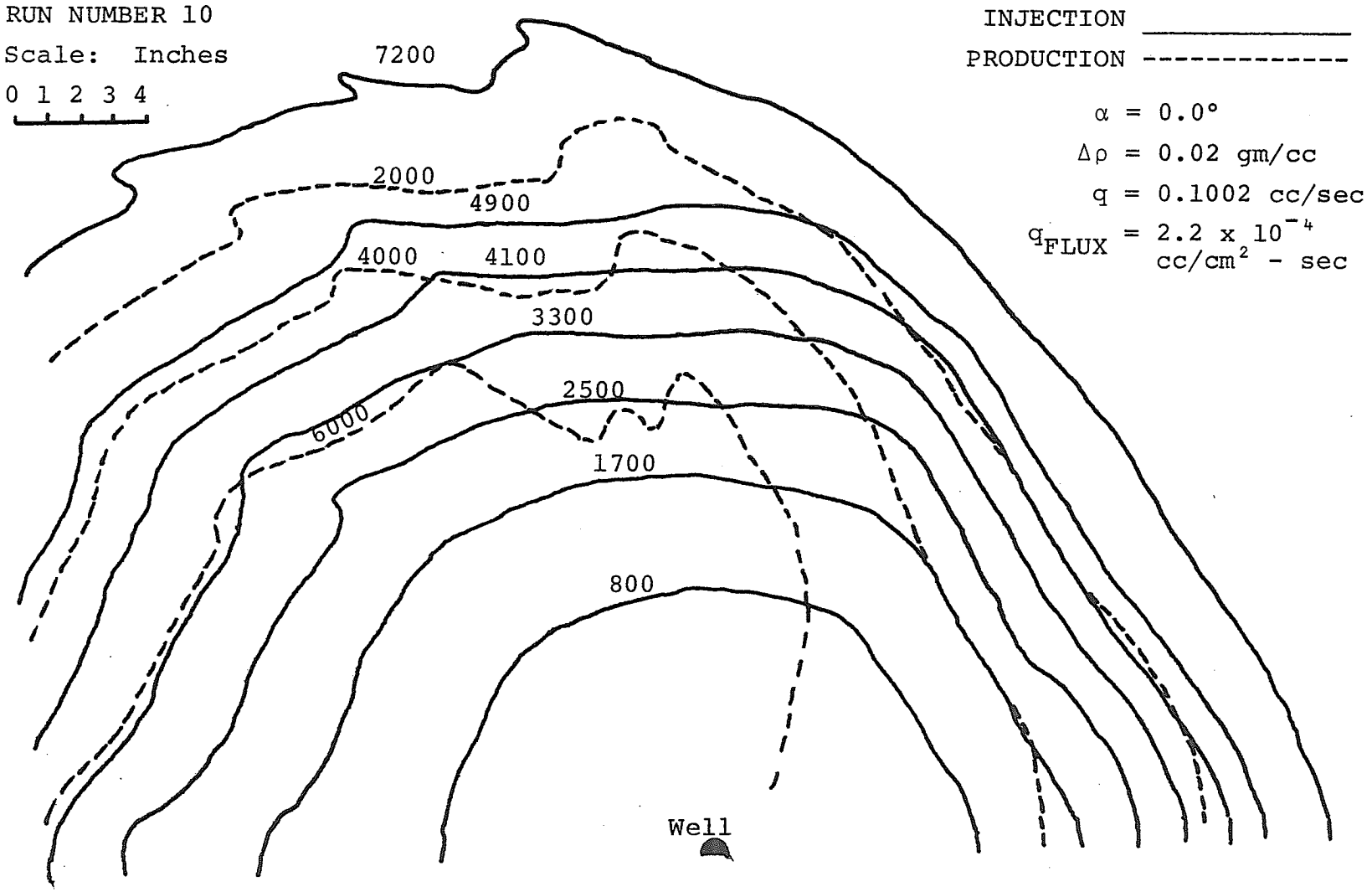
RUN NUMBER 10
Scale: Inches
0 1 2 3 4
INJECTION
PRODUCTION
α = 0.0°
Δρ = 0.02 gm/cc
q = 0.1002 cc/sec
q_{FLUX} = 2.2 x 10^{-4} cc/cm^2 - sec
7200
2000
4900
4000
4100
3300
2500
6000
1700
800
Well

RUN NUMBER 11

Scale: Inches

0 1 2 3 4

INJECTION _____

PRODUCTION ----------

$\alpha = 0.0°$

$\Delta\rho = 0.02$ gm/cc

$q = 0.06$ cc/sec

$q_{FLUX} = 6.1 \times 10^{-4}$ cc/cm^2 - sec

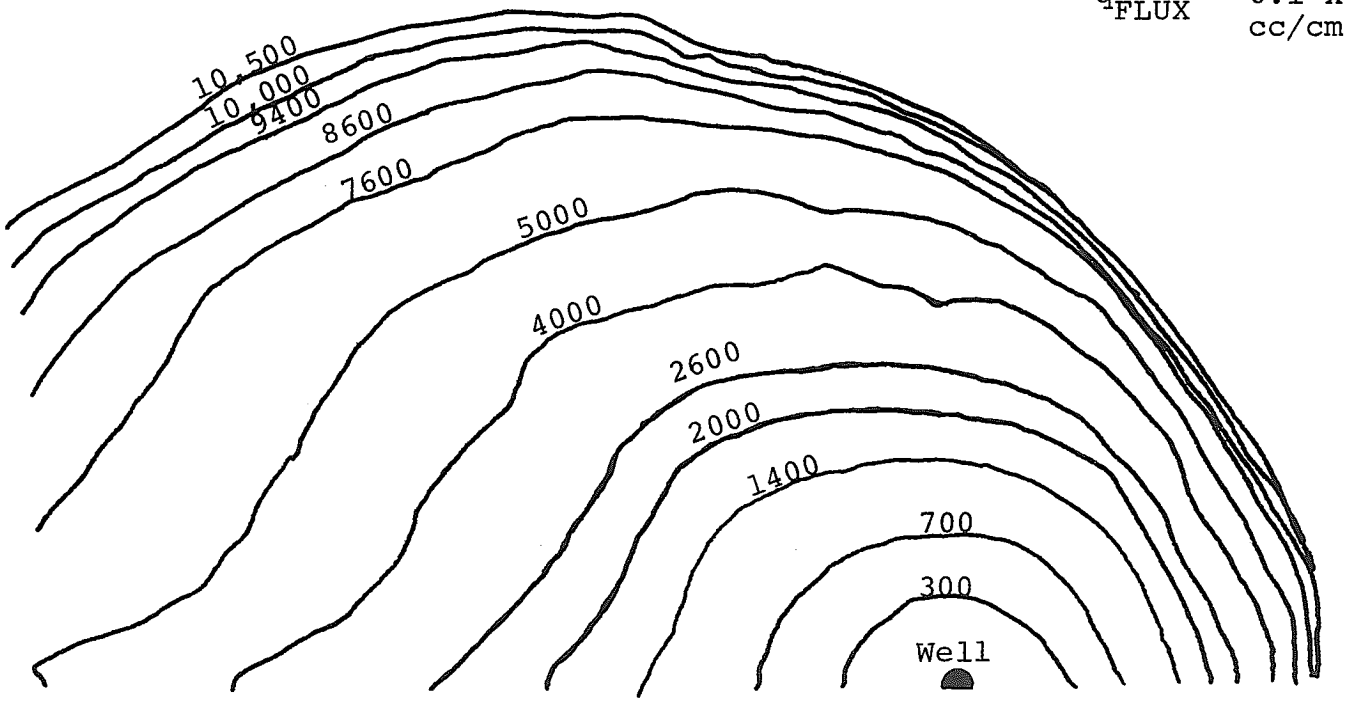

RUN NUMBER 12

Scale: Inches

0 1 2 3 4

INJECTION _____

PRODUCTION ----------

$\alpha = 0.0°$

$\Delta\rho = 0.017$ gm/cc

$q = 0.0668$ cc/sec

$q_{FLUX} = 0.84 \times 10^{-4}$ cc/cm^2 - sec

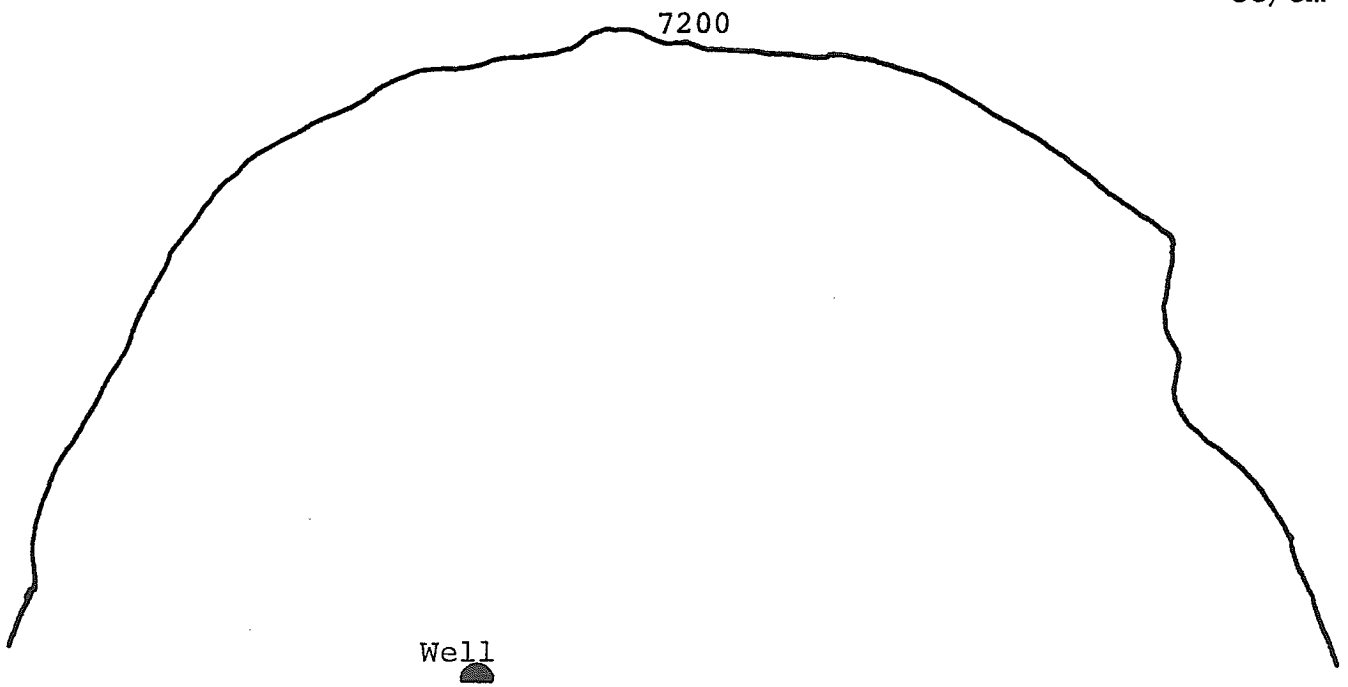

RUN NUMBER 13

Scale: Inches

0 1 2 3 4

INJECTION _____

PRODUCTION ----------

$\alpha = 0.0°$

$\Delta\rho = 0.021$ gm/cc

$q = 0.0668$ cc/sec

$q_{FLUX} = 0.25 \times 10^{-4}$ cc/cm^2 - sec

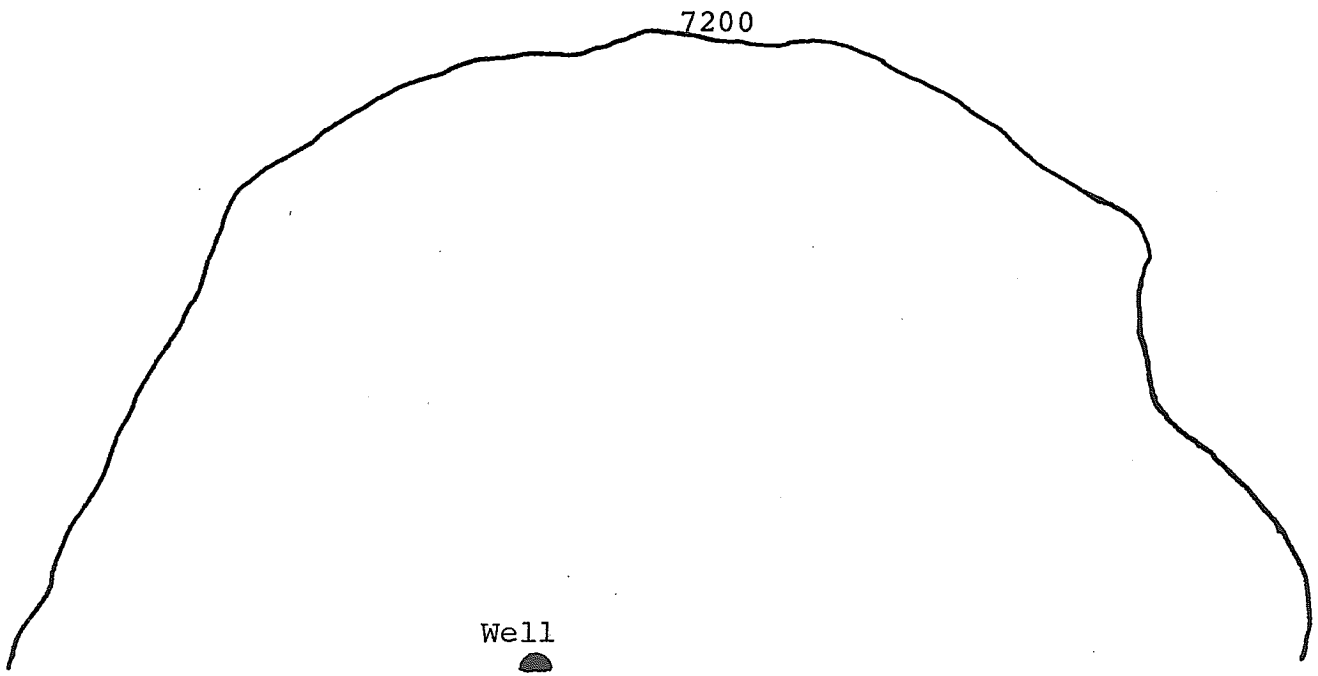

RUN NUMBER 14

Scale: Inches

0 1 2 3 4

INJECTION _____

PRODUCTION ----------

$\alpha = 15.0°$

$\Delta\rho = 0.210$ gm/cc

$q = 0.014$ cc/sec

$q_{FLUX} = 0.84 \times 10^{-4}$ cc/cm^2 - sec

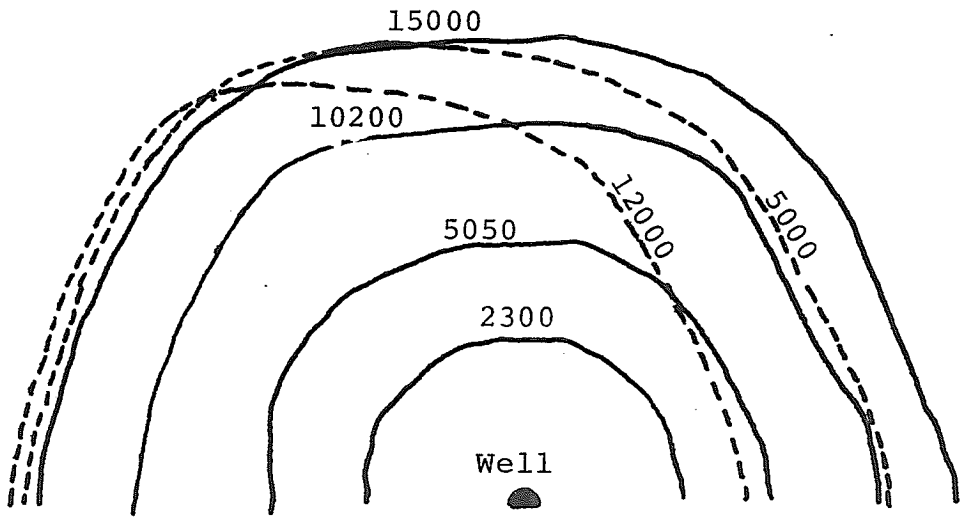

RUN NUMBER 15

Scale: Inches

0 1 2 3 4

INJECTION _____

PRODUCTION ----------

$\alpha = 15.0°$

$\Delta\rho = 0.22$ gm/cc

$q = 0.014$ cc/sec

$q_{FLUX} = 0.84 \times 10^{-4}$ cc/cm^2 - sec

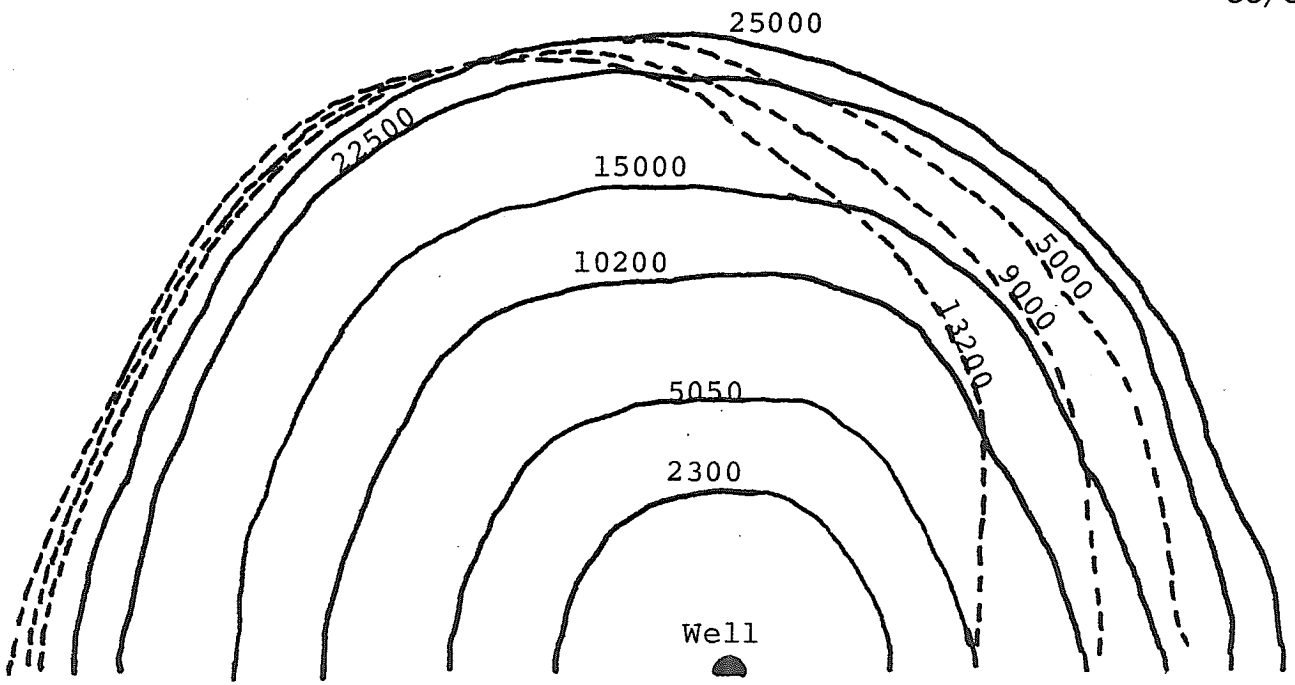

RUN NUMBER 16

Scale: Inches

0 1 2 3 4

INJECTION _____

PRODUCTION ----------

$\alpha = 15.0°$

$\Delta\rho = 0.23$ gm/cc

$q = 0.0140$ cc/sec

$q_{FLUX} = 0.84 \times 10^{-4}$ cc/cm^2 - sec

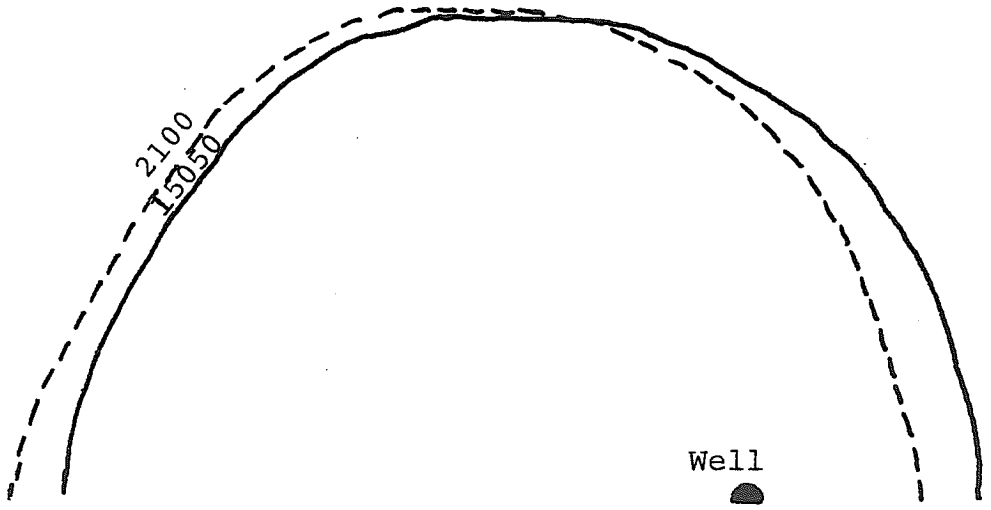

RUN NUMBER 17

Scale: Inches

0 1 2 3 4

INJECTION _____

PRODUCTION ----------

$\alpha = 30.0°$

$\Delta\rho = 0.215$ gm/cc

$q = 0.014$ cc/sec

$q_{FLUX} = 0.84 \times 10^{-4}$ cc/cm^2 - sec

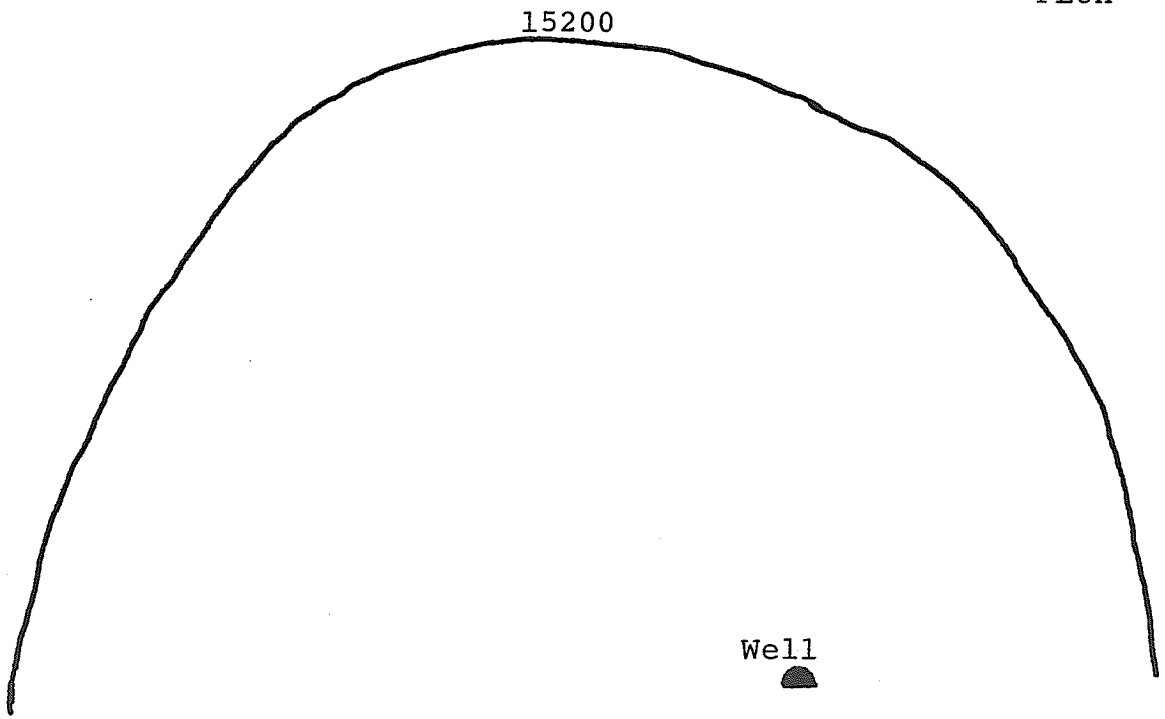

RUN NUMBER 18

Scale: Inches

0 1 2 3 4

INJECTION _____

PRODUCTION ----------

$\alpha = 30.0°$

$\Delta\rho = 0.21$ gm/cc

$q = 0.014$ cc/sec

$q_{FLUX} = 1.9 \times 10^{-4}$ cc/cm^2 - sec

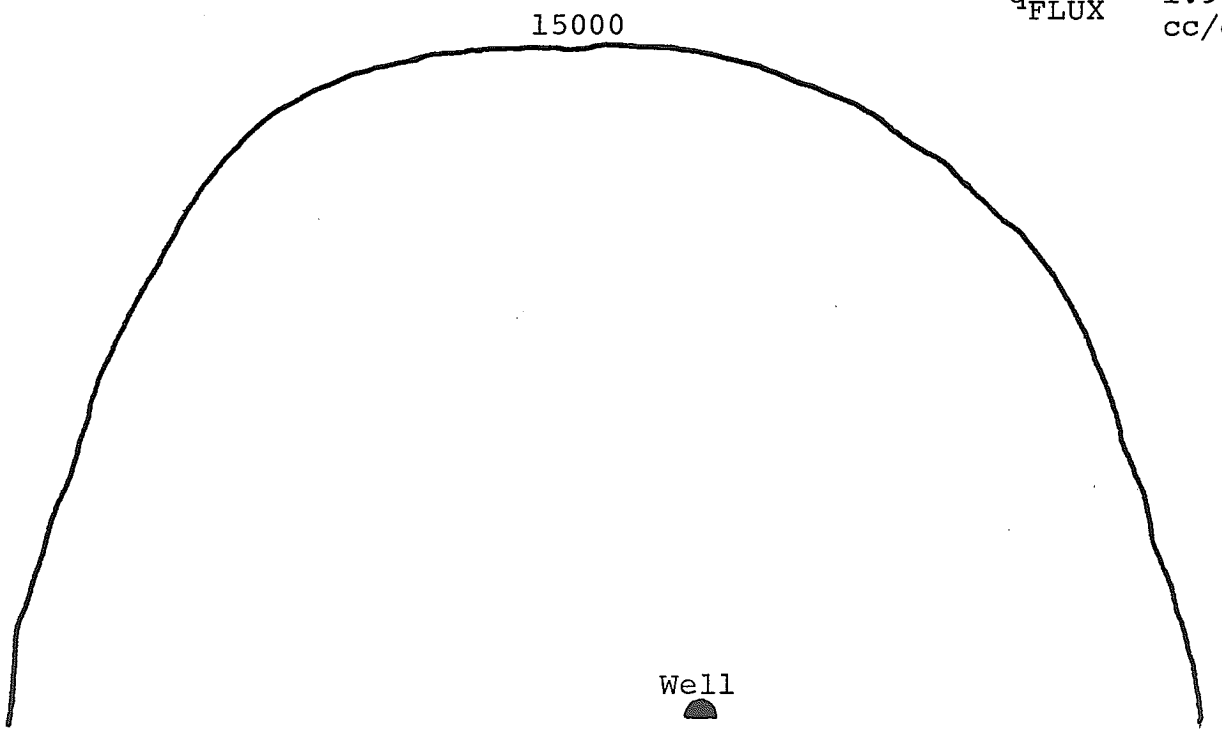

RUN NUMBER 19

Scale: Inches

0 1 2 3 4

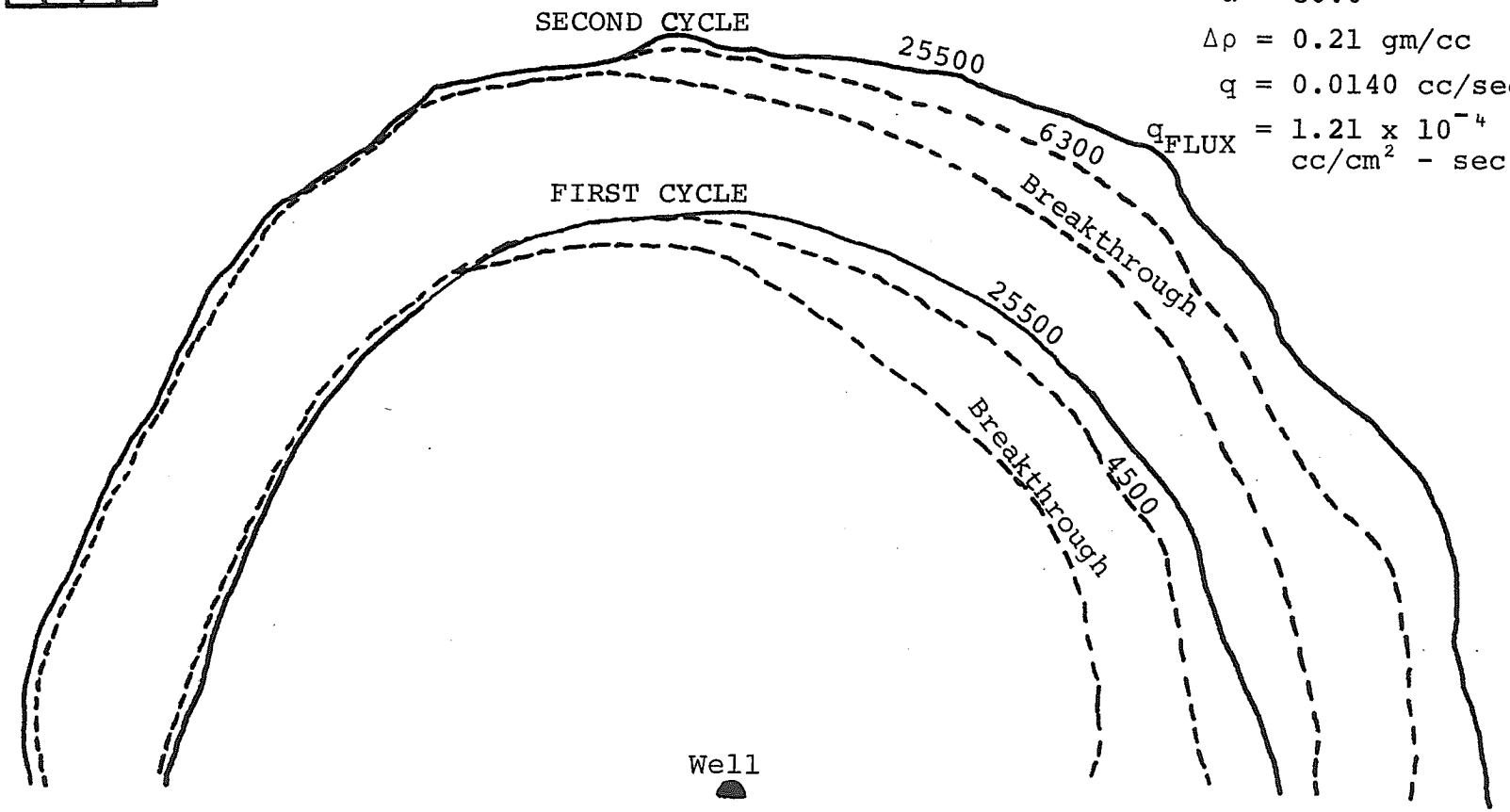

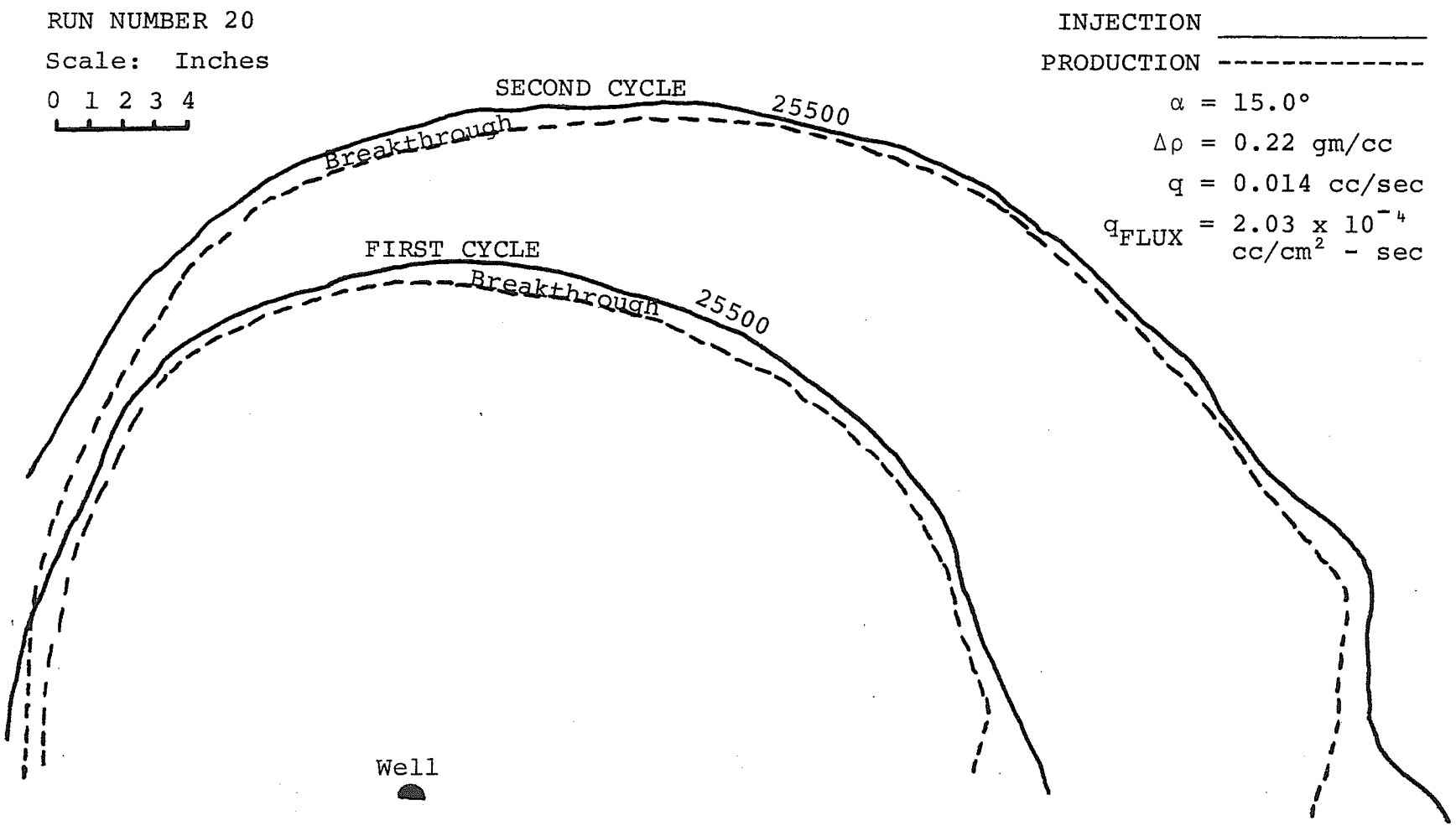
RUN NUMBER 20
Scale: Inches
0 1 2 3 4
SECOND CYCLE
Breakthrough
25500
FIRST CYCLE
Breakthrough
25500
Well
INJECTION
PRODUCTION
α = 15.0°
Δρ = 0.22 gm/cc
q = 0.014 cc/sec
q_{FLUX} = 2.03 x 10^{-4} cc/cm^2 - sec

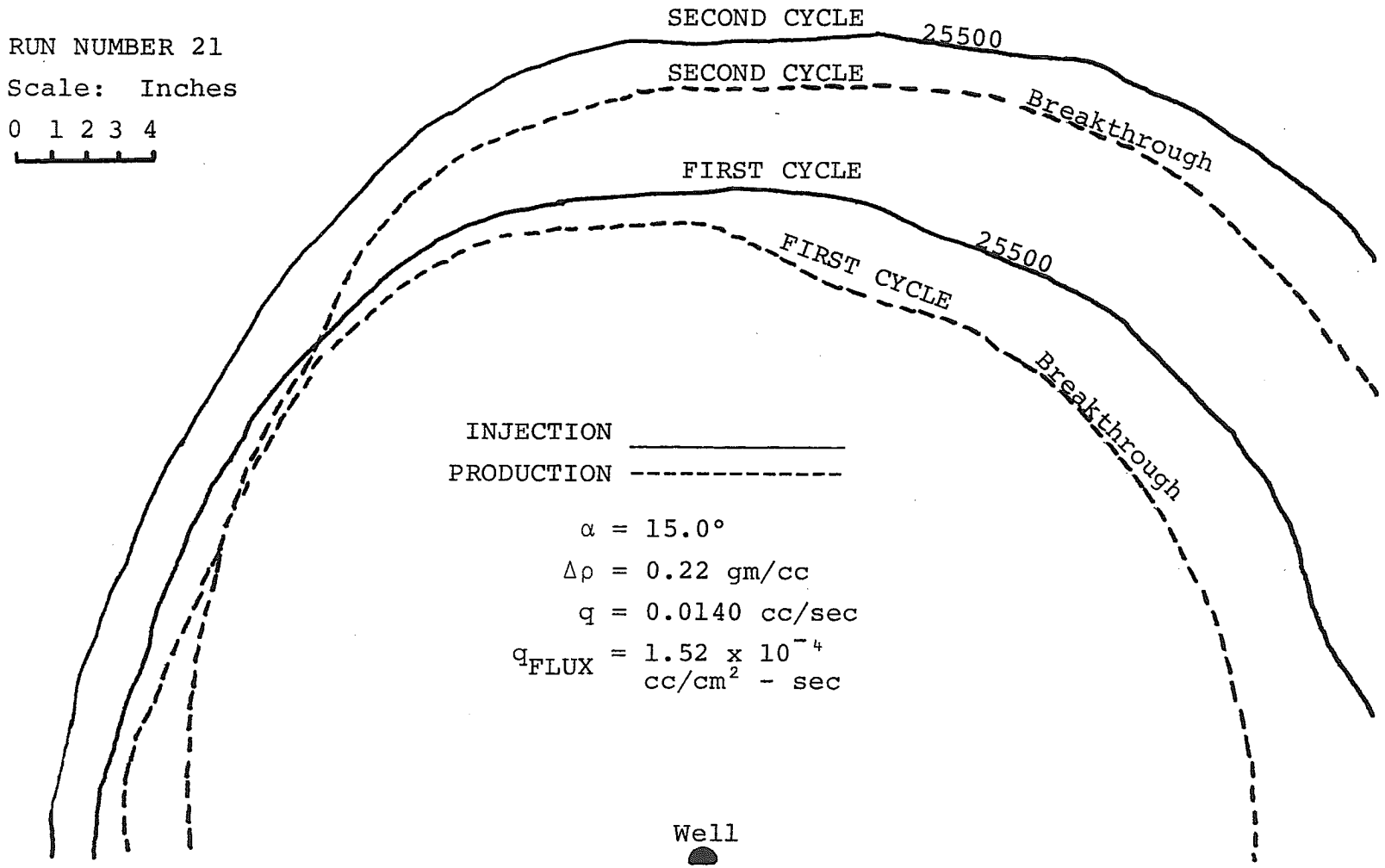
RUN NUMBER 21
Scale: Inches
0 1 2 3 4
SECOND CYCLE
25500
SECOND CYCLE
Breakthrough
FIRST CYCLE
25500
FIRST CYCLE
Breakthrough
INJECTION
PRODUCTION
α = 15.0°
Δρ = 0.22 gm/cc
q = 0.0140 cc/sec
q_{FLUX} = 1.52 x 10^{-4} cc/cm² - sec
Well

APPENDIX C

COMPUTER PROGRAM LISTING

C.1 Program Information

Title: AQUA I

Language: FORTRAN IV

System: IBM 360/65

Although the program is believed to be correct consistent with the assumptions and the approximations involved, neither the author, Louisiana State University, nor the Louisiana Water Resources Research Institute make any claims concerning its validity or correctness and anyone making use of the program does so at his own risk.

```
C
C     AQUA 1
C
C     WALID J. ESMAIL
C     LOUISIANA STATE UNIVERSITY,  BATON ROUGE
C     WATER RESOURCES  - 1973 -
C
C
C     THIS MATHEMATICAL MODEL CALCULATES THE RECOVERY EFFICENCY IN A
C     THIN THREE DIMENSIONAL MODEL FOR HORIZONTAL AND DIPPING SYSTEMS
C     WITH OR WITHOUT FLUX.
C     IT ASSUMES PISTON-LIKE DISPLACEMENT DURING THE INJECTION HALF
C     CYCLE. IT INCORPORATES LAYDOWN OF THE FRONT AT THE END OF THE
C     INJECTION HALF CYCLE, AND THE MIXED ZONE DURING THE PRODUCTION
C     HALF CYCLE. IT TRACKS TWO STREAMLINES ALONG THE LINE OF SYMMETRY
C     TO DETERMINE BREAKTHROUGH.
C
C    ***********************************************************************
C
C
C    *** LIST OF PARAMETERS USED IN THE MATHEMATICAL MODEL AQUA 1 ***
C
C
C    RESERVOIR PROPERTIES ***
C
C    XK = PERMEABILITY, DARCYS
C    VIS = VISCOSITY OF FLUID, CP
C    H = THICKNESS OF MODEL, CM.
C    POR = POROSITY, FRACTION
C    RW = WELLBORE RADIUS, CM.
C    RE = OUTER BOUNDARY RADIUS, CM.
C    ALF = DISPERSION COEFFICIENT FOR THE FLUID AND AQUIFER, CM.
C    DIFMOL = COEFFICIENT OF MOLECULAR DIFFUSION, SQ. CM./SEC.
C
C
C    RUN PARAMETERS ***
C
C    NO = RUN NUMBER
C    Q = INJECTION RATE , CC/SEC.
C    ALPHA = DIP ANGLE, DEGREES
C    DELRHO = DENSITY DIFFERENCE, GM/CC.
C    TINJ = INJECTION TIME, SEC.
C    TSTOR = STORAGE TIME, SEC.
C    FLINJ1 = FLUID INJECTED IN THE FIRST HALF CYCLE FOR FULL SYSTEM, CC.
C    QFLUX = FLUX RATE, CC/SEC.
C
C    TPV = TOTAL PORE VOLUME FOR HALF THE SYSTEM, CUBIC CM.
C    VI = INJECTED VOLUME FOR HALF CYCLE, CUBIC CM.
C    DPDX = POTENTIAL GRADIENT IN THE X DIRECTION, ATMOSPHERES/CM.
C    DPDY = POTENTIAL GRADIENT IN THE Y DIRECTION, ATMOSPHERES/CM.
C    VELX = VELOCITY IN THE X DIRECTION,CM./SEC.
C    VELY = VELOCITY IN THE Y DIRECTION,CM./SEC.
C    DELT = TIME INCREMENT PER COMPUTATIONAL STEP, SEC.
C    T = CUMMULATIVE INJECTION OR PRODUCTION TIME, SEC.
C    DRAG = EFFECT OF GRAVITY SEGREGATION ON THE VELOCITY IN THE X
C         DIRECTION,( EQ. 2.10) CM./SEC.
C    XCORR = FRONTAL LAYDOWN AT END OF INJECTION HALF CYCLE, CM.
C
```

```
C    NOL = NUMBER OF LAYERS
C    RINJ2
C    RINJ1 = RADIUS OF INJECTION DURING HALF-CYCLE, CM.(9INJ1-RINJ5)
C    R1 = RADIUS OF LEADING EDGE OF MIXED ZONE IN THE DI9ECTION OF MOVEMENT
C         FOR ANY HALF CYCLE, CM.
C    Q91 = INJECTION RATE FOR FIRST HALF CYCLE FOR FULL SYSTEM, CC/SEC.
C    QR2 = PRODUCTION RATE FOR FIRST PRODUCTION HALF CYCLE FO9 A FULL
C         SYSTEM, CC/SEC.
C    T1 TO T6 = ACTUAL TIME OF TRAVEL IN THE HALF CYCLE DENOTED BY
C         THE LAST NUMBER, SEC
C    FI1 = DENOMINATOR OF EQ.(2.14) IN KUMAR'S THESIS FO9 EACHHL
C    FI1 = DENOMINATOR OF EQ.(2.14) IN KUMAR'S THESIS FOR EACH HALF CYCLE
C    R2 = RADIUS OF LAGGING EDGE OF MIXED ZONE IN THE DIRECTION OF
C         MOVEMENT IN ANY HALF CYCLE, CM.
C    R3 = LENGTH OF THE MIXED ZONE, CM
C    QP = FLOW RATE PER CM, FOR EACH PRODUCTION HALF CYCLE
C    ERF = ERROR FUNCTION
C    C22 = CONCENTRATION AT THE ORIGINAL INTERFACE,(0.5), FRACTION
C    C11 = CALCULATED CONCENTRATION, VOL. FRACTION
C    RINC = LENGTH OF INCREMENT FOR CALCULATION OF MIXED ZONE, CM.
C    DG = DENSITY GRADIENT, GM./CM.**4
C    ACNG = ACCELERATION DUE TO GRAVITY, CM./SQ. SEC.
C    TST1 = TSTOR = STORAGE TIME, SEC.
C    DM1 = DIMENSIONLESS TIME GROUP (FIRST GROUP ON RIGHT SIDE OF EQ.(2.18)
C         OF KUMAR'S THESIS)
C    DM2 = DIMENSIONLESS GROUP  SECOND GROUP ON RIGHT SIDE OF EQ.(2.18))
C    X1 = PRODUCT OF DIMENSIONLESS GROUPS FOR THE FIRST INTERVAL
C    YL = RADIUS OF INTERFACE PROJECTION TO AQUIFER THICKNESS IN LINEAR
C         GEOMETRY ( LEFT SIDE OF EQ.(2.18) IN KUMAR'S THESIS)
C    YR = RATIO OF INTERFACE PROJECTION TO AQUIFER THICKNESSIN RADIAL
C         GEOMETRY ( LEFT SIDE OF KUMAR'S THESIS)
C         GEOMETRY ( LEFT SIDE OF EQ.(2.18) IN KUMAR'S THESIS)
C    XL = PROJECTION OF THE INTERFACE IN LINEAR GEOMETRY, CM.
C    XR = PROJECTION OF THE INTERFACE IN RADIAL GEOMETRY, CM.
C    T12D = ACTUAL TIME OF TRAVEL  ACROSS ANY ONE INTERVAL, DAYS
C    DELX = DISTANCE INCREMENT TO CALCULATE TIME PER COMPUTATIONAL STEP, CM.
C
C    CONVERSION FACTORS***
C
C    CFDSEC = CONVERSION FACTOR-FROM DAYS TO SECONDS
C    CFDSCM = CONVERSION FACTOR-FROM DARCYS TO CM.
C    CFFTCM = CONVERSION FACTOR-FROM FEET TO CM.
C
C
C
C    ************************************************************************
      DIMENSION X(55),Y(55),XIN(57),YIN(57)
      DIMENSION R(100),R2(100),R3(100)
      DIMENSION        C1(50),D1(50),XR(50),YR(50),A1(50),YL(50),B1(50),
     1XL(50),TS1D(50),TS1(53),XLFT(50),DG(500)
      DIMENSION A2(50),B2(50),C2(50),D2(50)
      DO 5050 I = 1,500
      XR(I) = 0.
      XL(I) = 0.
      YR(I) = 0.
      YL(I) = 0.
      A1(I) = 0.
      B1(I) = 0.
```

```
      C1(I) = 0.
      D1(I) = 0.
      TS1(I) = 0.0
      TS1D(I) = 0.
 5050 CONTINUE
C
C     READ RESERVOIR PROPERTIES
C
      READ(5,1500)XK,VIS,H,POR,RW,RE
C
C     WRITE RESERVOIR PROPERTIES
C
      WRITE(6,2500)XK,VIS,H,POR,RW,RE
C
      READ(5,901) ALF,DIFMOL
C
C     READ RUN PARAMETERS
C
    1 READ(5,2000,END= 999 )NO,Q,ALPHA,DELRHO,TINJ,TSTOR,FLINJ1,QFLUX
C
C     WRITE RUN PARAMTETERS
C
  105 WRITE (6,3000) NO,Q,ALPHA,DELRHO,TINJ,TSTOR,FLINJ1,QFLUX
C
C
      QR1 = 2.*Q
      QR2 = 2.*Q
      PPP = 3.14159*POR*H
      NOL=1
      TILN = 2.
      RINC = 0.10
C
C
C     PART1 - DEVELOPMENT OF MIXED ZONE DUE TO DIFFUSION AND DISPERSION
C     ----    ------------------------------------------------------
C
C     CALCULATION OF INTERVALS AND RADIUS IN EACH CYCLE
C
C     A-CALCULATION OF INTERVALS AND RADIUS OF INJECTION
C       IN INJECTION HALF CYCLE
C
      RINJ1=SQRT(FLINJ1/PPP)
      TNIN1=(RINJ1/TILN)
      NINT1=TNIN1
C
C     B-CALCULATION OF INTERVALS IN PRODUCTION HALF CYCLE
C
      NINT2=NINT1-1
      NTINT=NINT1+NINT2
      PRINT54,TILN   ,NTINT,NINT1,NINT2
C
C
      R4=(TILN/2.)
C
C     GENERATION OF RADII
C
      I=1
 796  IF(I.EQ.1)R(I)=TILN
```

```
      IF(I.GT.1)R(I)=R(I-1)+TILN
      GOTO21
  797 IF(I.GT.NTINT) GO TO 1010
      IF((I-1).LE.2)R(I)=TILN
      IF((I-1).GT.2)R(I)=R(I-1)-TILN
C
C     GENERATING THE TERMS OF EQUATION 11
C     ONE INJECTION-PRODUCTION CYCLE
C
 21   IF(I-NINT1)18,18,190
 18   R5=R(I)-R4
      R1=R5-RW
      T1=PPP    *((R5)**2-(RW)**2)/(QR1)
      IF(T1)2001,2001,3001
 3001 QI1=QR1/(2.*PPP    )
      FI1=1.333*ALF*(2.*QI1*T1)**1.5+DIFMOL*(2.*QI1*T1)**2/QI1
 200  Z=(QI1*T1-(R1**2)/2.)/FI1**.5
      GOTO202
 190  R5=R(I)+R4
      R1=R5-RW
      T1=PPP    *(R(NINT1)**2-(RW)**2)/(QR1)
      T2=T1+PPP    *(R(NINT1)**2-R5**2)/(QR2)
      QP2=QR2/(2.*PPP    )
      FP2=1.333*ALF*((2.*QP2*T2)**1.5+(2.*QI1*T1)**1.5-(2.*QP2*
     1T1)**1.5)+
     2DIFMOL*((2.*QP2*T2)**2/QP2+(2.*QI1*T1)**2/QI1-(2.*QP2
     3*T1)**2/QP2)
 201  Z=(-QP2*T2-(R1**2)/2.+QI1*T1+QP2*T1)/FP2**.5
C
C     CALCULATION OF ERROR FUNCTION BY TABLE LOOK UP
C
 202  EC=1.-ERF(Z)
C
C
C     CALCULATIONS OF CONCENTRATIONS & MIXED ZONE LENGTHS R3
C
      C22 = 0.5
 242  C11=0.5*EC
      IF(C11 - C22)104,104,6
  104 IF(I.GT.NINT1.AND.R1.LT.RINC)GO TO 1010
      IF(C11- .03) 556,556,557
 556  R2(I)=R1
      GOTO220
 557  R1=R1-RINC
 402  IF(I-NINT1)200,200,201
 220  R1=R5+RINC
 403  IF(I-NINT1)200,200,201
 6    IF(C11-.97)7,8,8
 7    R1=R1+RINC
 406  IF(I-NINT1)200,200,201
 8    R3(I)=R1-R2(I)
      DG(I) = DELRHO/R3(I)
      WRITE(6,553) I,R1,R2(I),R3(I),DG(I)
      ACNG = 981.
      CFDSEC=24.*60.*60.
      CFDSCM=(.987E-8)
 53   CFFTCM=30.48
      TST1 = TSTOR
```

```
C
C
C
C     PART 2 - DEVELOPMENT AND PROJECTION OF INTERFACE DUE TO
C     ----     ---------------------------------------------
C               GRAVITY SEGREGATION
C               ------------------
C
C
C
C
C     CALCULATION OF DIMENSIONLESS GROUP
C
      VISC = VIS/100.
      DM1 = (XK*CFDSCM*ACNG*DELRHO)/(POR*VISC*H)
      DM2 = ((VISC**.66*DG(I))/(DELRHO**1.66*ACNG**.33))
      PRINT333,I,DM1,DM2
C
C     CALCULATION OF THE PROJECTION OF THE FIRST INTERVAL
C
      IF(I-1)80,80,81
 80   T11=(PPP    *(R(I)**2-(RW)**2))/QR1
 51   X1=(DM1*T11)*(DM2**.5)
      IF(X1-0.1)71,71,61
 61   YL(I)=0.8379+11.688*X1-4.19*X1**2
      GOTO56
 71   YL(I)=19.67*X1+.033
 56   XL(I)=YL(I)*H
      T11D=T11/CFDSEC
      PRINT550,I,T11D,X1,I,XL  (I)
      GOTO29
C
C     CALCULATION OF PSEUDO-TIME AND PROJECTION OF THE INTERFACE
C     WHERE EQUATION (17) IS APPLICABLE
C
 81   IF(I-NINT1)82,82,83
 82   T12=(PPP    *ABS(R(I)**2-R(I-1)**2))/QR1
      GOTO84
 83   T12=(PPP    *ABS(R(I)**2-R(I-1)**2))/QR2
 84   IF(YL(I-1)-2.)101,101,102
 102  CQ=-.8379+YL(I-1)
      BQ=11.688*DM1*(DM2**.5)
      AQ=4.19*(DM1**2)*DM2
      TSP1=(BQ-SQRT(BQ**2-4.*AQ*CQ))/(2.*AQ)
      TT1=T12+TSP1
 811  IF(I-NINT1)307,306,307
 307  X2=(DM1*TT1)*(DM2**.5)
      GOTO308
 306  TS1(I)=TT1 + TST1
      X2=(DM1*TS1(I))*(DM2**.5)
 308  YL(I)=.8379+11.688*X2-4.19*X2**2
 582  XL(I)=YL(I)*H
      TS1D(I)=TS1(I)/CFDSEC
      T12D=T12/CFDSEC
      TSP1D=TSP1/CFDSEC
      TT1D=TT1/CFDSEC
      XLFT(I)=XL(I)/CFFTCM
      IF(I.EQ.NINT1)PRINT114,I,TS1D(I)
```

```
      WRITE(6,111) I,T12D,TSP1D,TT1D,I,YL(I),I,XLFT(I)
      GOTO29
C
C     CALCULATIONS OF THE PSEUDO-TIME AND PROJECTION OF THE INTERFACE
C     FOR THE CASE WHERE EQUATION (16) IS USED
C
 101  AL=(YL(I-1)-.033)/19.67
      AL2=DM1*(DM2**.5)
      TSP2=AL/AL2
      TT2=T12+TSP2
 812  IF(I-NINT1)298,299,298
 298  X3=(DM1*TT2)*(DM2**.5)
      GOTO301
 299  TS1(I)=TT2+TST1
      X3=(DM1*TS1(I))*(DM2**.5)
 301  YL(I)=19.67*X3+.033
 303  XL(I)=Y_(I)*H
      TS1D(I)=TS1(I)/CFDSEC
      T12D=T12/CFDSEC
      TSP2D=TSP2/CFDSEC
      TT2D=TT2/CFDSEC
      XLFT(I)=XL(I)/CFFTCM
      WRITE(6,112) I,T12D,TSP2D,TT2D,I,YL(I),I,XLFT(I)
      IF(I.EQ.NINT1)PRINT115,I,TS1D(I)
C
C
 29   I=I+1
 768  IF(I-NINT1)796,796,797
C
 1010 CONTINUE
C
C     PART 3 - CORRECTION TO RADIAL GEOMETRY
C              ------------------------------
C
C
C
C     CORRECTION TO RADIAL GEOMETRY (INJECTION HALF CYCLE)
C
C
  950 WRITE(6,909)
      L = I-1
C
      DO888 I=1,NINT1
 70   IF(R(I)-TILN)30,30,35
 30   XR(I)=XL(I)
      GOTO444
 35   A1(I)=3.14*((R(I-1)+.5*XR(I-1))**2-R(I-1)**2)
      B1(I)=3.14*(R(I-1)**2-(R(I-1)-.5*XR(I-1))**2)
      C1(I)=SQRT((A1(I)+3.14*R(I)**2)/3.14)
      D1(I)=SQRT((3.14*R(I)**2-B1(I))/3.14)
      XR(I)=(C1(I)-D1(I))+(XL(I)-XL(I-1))
 444  YR(I)=XR(I)/H
      WRITE(6,40) I,XR(I),YR(I)
 888  CONTINUE
C
10000 CONTINUE
C
C
```

```
C
C     PART 4   CALCULATION OF RECOVERY EFFICIENCY
C              ------------------------------------
C
C
      WRITE(6,98)
C
C     INITIALIZE ACCUMULATORS & ARRAY AREAS
C
      VIMAX=0.0
      T=0.0
      DELX = 0.5
      NN = TILN/DELX
      FLUXGR = -(QFLUX*VIS)/(XK*110.*H)
      C=9.672E-04*XK*DELRHO*SIN(ALPHA*3.14159/180.)/(VIS*POR)
      TPV=3.14159*RE**2*H*POR/2.0
      VI=3.14159*RW**2*H/2.
      SIGN=1.0
C
C     NO. STREAMLINES (NS)
C
      NS = 2
      K = NINT1 + 1
      NSM1=NS-1
      DO 5 I=1,NS
      X(I)=0.0
      Y(I)=0.0
    5 CONTINUE
C     COMPUTE INITIAL STARTING POINTS
      DO 10 I=1,NS
      XI=I
      X(I)=RW*COS(3.14159*(XI-1.0)/NSM1)
      Y(I)=RW*SIN(3.14159*(XI-1.0)/NSM1)
   10 CONTINUE
C
C     POINT SOURCE-SINK POTENTIAL DISTRIBUTION FORM OF STEADY-STATE
C     RADIAL FLOW EQATION
C
      WRITE(6,106)
   19 QD=-Q*VIS/(3.14159*XK*H)
      J = 0
 22   J = J+1
   20 DO 100 I=1,NS
      DPDX = (QD*X(I)/(X(I)**2+Y(I)**2))+FLUXGR
      DPDY=QD*Y(I)/(X(I)**2+Y(I)**2)
      VE_X=-XK*DPDX/(VIS*POR)
      VELY=-XK*DPDY/(VIS*POR)
      IF(I.EQ.1)VELY=0.0
      IF(I.EQ.NS)VELY=0.0
      IF(I.EQ.1)DELT=DELX/SQRT(VELX**2)
      IF((T+DELT).GT.TINJ.AND.SIGN.GT.0.0)DELT=TINJ-T
      Y(I)=Y(I)+VELY*DELT
      IF(I.EQ.NS)Y(I)=0.0
      IF(I.EQ.1)Y(I)=0.0
C
C     SUPERIMPOSITION OF GRAVITATIONAL EFFECTS
C
      DUMMY = VI/TPV
```

```
      IF(DUMMY.LT.0.)WRITE(6,877) VI,TPV
      DRAG = (VI/TPV)**0.17
      VCORR=VELX-C*DRAG
      X(I)=X(I)+VCORR*DELT
C
C     WRITE X COORDINATES OF THE STREAMLINES
C
      WRITE(6,113) I,X(I)
C
C     THE FOLLOWING CHECKES ON BREAKTHROUGH FOR BOTH STREAMLINES
C
      IF(X(NS).GT.0.0.OR.X(1).LT.0.0) GO TO 1000
      IF(Q.GT.0.0) GO TO 100
      DUMMY1 = X(1) - R3(K)/2.
      DUMMY2 = ABS(X(NS)) - R3(K)/2.
      IF(DUMMY1.LT.RW.OR.DUMMY2.LT.RW) GO TO 1000
C
  100 CONTINUE
C
      T = T+DELT
      IF(Q.GT.0.0)VI=Q*T
      IF(Q.LT.0.0)VI=VIMAX+Q*T
      IF(VI.GT.VIMAX)VIMAX=VI
      IF(T.LT.TINJ.AND.SIGN.GT.0.0)GO TO 20
C
C     PRODUCTION CYCLE
C     PRODUCTION CYCLE TERMINATED WHEN FIRST STREAMLINE INTERSECTS WELLBORE
C
      IF(T.EQ.TINJ.AND.SIGN.GT.0.0) GO TO 68
      IF(J.EQ.NN) GO TO 908
      GO TO 22
  908 IF(K-L) 66,66,1000
   66 DUM1 = X(1) - R3(K)/2.
      DUM2 = ABS(X(NS)) - R3(K)/2.
      IF(DUM1.LE.RW.OR.DUM2.LE.RW) GO TO 1000
      K = K+1
      J = 0
      GO TO 22
C
C     STORAGE TIME CALCULATIONS
C     X-POSITIONS UPDATED FOR TIME OF STORAGE
C
   68 IF(TSTOR.EQ.0.0) GO TO 300
      VSTOR=C*DRAG
      DO 209 I=1,NS
      X(I)=X(I)-VSTOR*TSTOR
  209 CONTINUE
      WRITE(6,4000)TSTOR
  300 CONTINUE
C
C     INJECTION HALF CYCLE TERMINATES , PRODUCTION HALF CYCLE STARTS
C
      T=0.0
      SIGN=-1.0
      Q=-ABS(Q)
      WRITE(6,5000)
C
C   FRONTAL LAYDOWN
```

```
C
      IF(ALPHA.LT.2.) GO TO 771
      A = (90.-ALPHA)*3.14159/180.
      XCORR = (SIN(A)/COS(A))*0.5
      IF(XR(NINT1).LT.XCORR) GO TO 771
      GO TO 772
  771 XCORR = XR(NINT1)
  772 DO 2 I = 1,1
      X(I) = X(I) - XCORR
    2 CONTINUE
      DO 3 I = 2,NS
      X(I) = -(ABS(X(I))-XCORR)
    3 CONTINUE
      J = 0
      GO TO 19
 1000 CONTINUE
C
C     RECOVERY EFFICIENCY (REC)
C
      REC = 2.*T*ABS(Q)/FLINJ1
      WRITE(6,5500)REC
C
      GO TO 1
C
C     FORMAT STATEMENTS
C
   98 FORMAT(1H1)
  901 FORMAT(2F15.8)
   54 FORMAT(///6X,10HINTERVALS / ,
     1  9X,28HLENGTH OF EACH INTERVAL (CM),20X,F 5.2/,
     2  9X,25HTOTAL NUMBER OF INTERVALS,22X,I4/,
     3  9X,33HINTERVALS IN INJECTION HALF CYCLE,14X,I4/,
     4  9X,34HINTERVALS IN PRODUCTION HALF CYCLE,13X,I4/,
     5 1H1,58X,10HP A R T  2/58X,12H----------///,
     6      45X,37HCALCULATIONS FOR INJECTION HALF CYCLE/,
     7      44X,39H---------------------------------------///)
  877 FORMAT(///10X,'VI =',E15.6,10X,'TPV =',E15.6)
  130 FORMAT(/5X,'FLUXGR =',F10.8,3X,'DPDX =',F10.8,3X,'DPDY=',F10.8)
   40 FORMAT(//5X,'I = ',I2,5X,'XR(I) = ',E15.8,5X,'YR(I) = ',E15.8)
  909  FORMAT(1H1,53X,10HP A R T  3///,
     1 32X,52HCORRECTION TO RADIAL GEOMETRY(INJECTION  HALF CYCLE)/,
     2 31X,53H-----------------------------------------------------///)
  115  FORMAT(80X,5HTS1D(,I3,2H)=,E15.8,///,
     1  1H1,40X,41HCALCULATIONS DURING PRODUCTION HALF CYCLE/,
     2       40X,43H-------------------------------------------///)
  112  FORMAT(1X,2HI=,I3,3X,5HT12D=,E15.8,3X,6HTSP2D=,E15.8,4X,5HTT2D=,
     1E15.8,2X,3HYL(,I3,2H)=,E15.8,1X,5HXLFT(,I3,2H)=,E15.8///)
  553 FORMAT(/  ,1X,'I=',I3,3X,'R1=',E15.8,3X,'R2(I)=',E15.8,3X,'R3(I)='
     2,E15.8,5X,'DG(I) =',E15.8)
  114  FORMAT(80X,5HTS1D(,I3,2H)=,E15.8///,
     1 1H1,40X,41HCALCULATIONS DURING PRODUCTION HALF CYCLE/,
     2      40X,43H-------------------------------------------///)
  111  FORMAT(1X,2HI=,I3,3X,5HT12D=,E15.8,3X,6HTSP1D=,E15.8,4X,5HTT1D=,
     1E15.8,2X,3HYL(,I3,2H)=,E15.8,1X,5HXLFT(,I3,2H)=,E15.8///)
  550  FORMAT(1X,2HI=,I3,3X,5HT11D=,E15.8, 6X,3HX1=,E15.8,50X,5HXL  (,I3,
     12H)=,E15.8///)
  333  FORMAT(1X,2HI=,I3,4X,4HDM1=,E15.8,5X,4HDM2=,E15.8)
  106 FORMAT(1H1//15X,'INJECTION HALF CYCLE',//,15X,'STREAMLINE TRACKING
```

```
     1',//)
  113 FORMAT(5X,'X(',I2,') =',2X,F10.5)
 1500 FORMAT (6F10.5)
 2000 FORMAT (I2,F13.5,F5.0,F5.2,F10.0,F5.1,F10.4,F10.7)
 2500 FORMAT(1H1,50X,'RESERVOIR PROPERTIES',///12X,'PERMEABILITY',21X'VI
     1SCOSITY',26X,'THICKNESS',23X,'POROSITY',/,13X,'(DARCIES)',26X,'(CP
     2)',31X,'(CM)',26X,'(FRAC)',///,15X,F5.2,28X,F5.3,29X,F7.1,24X,F5.3
     3,////,35X,'WE_LBORE RADIUS',30X,'DRAINAGE RADIUS',/,40X,'(CM)',42X
     4,'(CM)'///,39X,F5.2,40X,F6.1)
 3000 FORMAT(1H1/////,54X,'-RUN NUMBER ',I2,' -',////10X,'INJECTION RATE
     1(CC/SEC)=',F7.5,57X,'DIP ANGLE(DEG)=',F9.2,//10X,'DENSITY DIFF.(GM
     2/CC)=',F7.3,59X,'INJ. CYCLE(SEC)=',F6.0,//,10X,'STORAGE TIME(SEC)=
     3',F7.0,62X,'FLUID INJECTED(CC)=',F10.5,//,49X,'FLUX RATE(CC/SEC)='
     4,F10.7)
 4000 FORMAT(1H1,////////////////////,50X'STORAGE TIME(SEC)',//53X,E11.5)
 5000 FORMAT(1H1,////////////////////,55X,'PRODUCTION CYCLE')
 5500 FORMAT(////,50X,'RECOVERY EFFICIENCY = ',F4.2)
  999 CONTINUE
 2001 WRITE(6,2002)
 2002 FORMAT(10X,49HRADIUS OF FIRST FRONTAL POSITION IS LESS THAN THE/,
     1  16HWELL BORE RADIUS)
      STOP
      END
```

APPENDIX D

COMPUTER PROGRAM LISTING

D.1 Program Information

Title: PLOT I

Language: FORTRAN IV

System: IBM 360/65

Although the program is believed to be correct, neither the author, Louisiana State University, nor the Louisiana Water Resources Research Institute make any claims concerning its validity or correctness and anyone making use of the program does so at his own risk.

```
C
C
C    WALID J. ESMAIL
C
C    LOUISIANA STATE UNIVERSITY   BATON ROUGE
C
C    WATER RESOURCES - FALL, 1972
C
C
C
C    THIS PROGRAM TRACKS AND PLOTS TEN STREAMLINES IN A HORIZONTAL
C    SYSTEM INCORPORATING TEN IMAGE WELLS. IT ACCOMODATES FLUX AS WELL.
C
C
C    PARAMETERS USED IN THIS PROGRAM ARE
C
C    Q = INJECTION RATE - CUBIC CM. PER SECOND
C    VISC = VISCOSITY - CP.
C    H = THICKNESS - CM.
C    PERM = PERMEABILITY - DARCYS
C    POR = POROSITY - FRACTION
C    C2 = PRESSURE GRADIENT DUE TO FLUX - ATMOSPHERS PER CM.
C    DELT = TIME INCRUMENT - SECONDS
C    NSL = NUMBER OF STREAMLINES
C    RSTART = STARTING POINT - CM.
C
C
      DIMENSION XCOORD(10,400),YCOORD(10,400),JCOUNT(10)
      DIMENSION DELT(10,400),ET(10,400),TIME(10),X(1000),Y(1000)
      DIMENSION PSPACE (8000)
C
      READ(5,1) Q,VISC,H,PERM,C2
    1 FORMAT(5F15.10)
      READ(5,2) RSTART,SDELT,NSL,POR
    2 FORMAT(2F10.5,I5,F10.5)
C
      WRITE (6,98)
   98 FORMAT(1H1,////////,28X,'D A T A',//)
      WRITE (6,99)Q,VISC,H,PERM,C2,RSTART,SDELT,NSL,POR
   99 FORMAT(10X,'INJECTION RATE =',F10.8,2X,'CC PER SECOND',//,10X,'VIS
     1COSITY =',F5.3,2X,'CP',//,10X,'THICKNESS =',F5.3,2X,'CM.',//,
     210X,'PERMEABILITY =',F5.3,2X,'DARCYS',//,10X,'PRESSURE GRADIENT ='
     3,F12.10,2X,'ATMOSPHERES PER CM.',//,10X,'STARTING POINT =',F5.3,2X
     4,'CM.'//10X,'INITIAL TIME INCRIMENT =',F5.3,2X,'SECONDS'//10X,'NUM
     5BER OF STREAMLINES =',I3,//,10X,'POROSITY =',F5.3////)
C
      C1 = -((Q*VISC)/(2.*3.14159*PERM*H))
      C3 = -(PERM/(POR*VISC))
      XSTOP = -C1/C2
      WRITE (6,3) XSTOP
    3 FORMAT(10X,'FRONT STOPS AT X =',F6.3,',Y=0.0')
C
C    COMPUTE THE DIMENSIONLESS COORDINATES OF THE STARTING POINTS FOR THE
C    STREAMLINES
C
      ANSL = NSL -1
      THETA = 3.14159/ANSL
      RW = 0.625
```

```
      J = 1
      DO 25 I = 1,NSL
      XCOORD(I,J) = RSTART*COS((NSL-I)*THETA)
      YCOORD(I,J) = RSTART*SIN((NSL-I)*THETA)
   25 CONTINUE
C
C
C    TRACE THE STREAMLINES
C
      I = 1
   29 ET(I,J) = 0.0
      DELT(I,J) = SDELT
   30 XC = XCOORD(I,J)
      YC = YCOORD(I,J)
      VAL1 = XC**2 + YC**2
      SUMX = 0.
C
C    THE FOLLOWING SUMS THE DIMENSIONLESS FORMS OF THE POTENTIAL
C    GRADIENT EQUATION TO BE USED IN THE SUBROUTINE TO CALCULATE THE
C    POTENTIAL GRADIENTS IN THE X AND Y DIRECTIONS.
C    THE '5' REPRESENTS THE NUMBER OF IMAGE WELLS ON EACH END.
C
      DO 19 N = 1,5
      XN = N
   19 SUMX=SUMX+(XC/(XC **2+((YC-(220.*XN))**2)))+(XC/(XC**2+((YC+(220.*
     1XN))**2)))
      SUMY = 0.
      DO 21 N = 1,5
      XN = N
   21 SUMY =SUMY+(YC-(220.*XN))/(XC**2+((YC-(220.*XN))**2))+(YC+(220.*
     2XN))/(XC**2+((YC+(220.*XN))**2))
C
      CALL PGRAD(C1,C2,XC,YC,VAL1,SUMX,SUMY,PGRADX,PGRADY)
      J = J+1
C
      DELX = C3*PGRADX*DELT(I,(J-1))
      DELY = C3*PGRADY*DELT(I,(J-1))
      DELR = SQRT(DELX**2 +DELY**2)
C
      IF(J-400) 31,31,56
   31 XCOORD(I,J)= XCOORD(I,(J-1))+DELX
      YCOORD(I,J) = YCOORD(I,(J-1))+DELY
C
      ET(I,J) = ET(I,(J-1))+ DELT(I,(J-1))
      IF(DELR.LT.0.5) DELT(I,J) = 2.*DELT(I,(J-1))
      IF(DELR.GE.0.5) DELT(I,J) = DELT(I,(J-1))
C
      IF(ABS(XCOORD(I,J)).GE.110.OR.YCOORD(I,J).GE.110.) GO TO 50
      IF(I.EQ.1) TCHECK = ET(I,J)
      IF(ET(I,J).GT.TCHECK) GO TO 50
      JCOUNT(I) = J
      GO TO 30
   50 I = I+1
      IF(I-NSL) 55,55,60
   55 J = 1
      GO TO 29
C
   56 WRITE (6,57) I
```

```
   57 FORMAT(10X,31HDIMENSION EXCEEDED , STREAMLINE,I2)
C
      GO TO 50
   60 DO 75 I = 1,NSL
C
      WRITE (6,65)
   65 FORMAT(1H1,10X,'STREAMLINE',5X,'TIME STEP',5X,'STEP NUMBER',5X,'
     1XCOORD',5X,'YCOORD',5X,'ELAPSED TIME'/)
C
      JINDEX = JCOUNT(I)
      DO 75 J = 1,JINDEX
      WRITE (6,70) I,DELT(I,J),J,XCOORD(I,J),YCOORD(I,J),ET(I,J)
   70 FORMAT(14X,I2,12X,F8.0,10X,I3,9X,F9.4,3X,F8.4,5X,F8.0)
   75 CONTINUE
C
C
C    PLOTTING THE STREAMLINES
C
      CALL PLOTS(PSPACE,8000)
      CALL PLOT (12.,-40.,-3)
      CALL PLOT(0.,1.,-3)
      CALL SYMBOL (0.,0.,0.07,3.0.,-1)
      DO 90 I = 1,NSL
      JINDEX = JCOUNT(I)
      DO 80 J = 1,JINDEX
      X(J) = XCOORD(I,J)
      Y(J) = YCOORD(I,J)
   80 CONTINUE
      J1 = JINDEX + 1
      J2 = JINDEX + 2
      X(J1) = 0.
      X(J2) = 14.
      Y(J1) = 0.
      Y(J2) = 14.
      CALL LINE (X,Y,JINDEX,1,0,0)
   90 CONTINUE
C
C
C
C    TERMINATING CALLS
C
      CALL PLOT(0.,12.,-3)
      CALL PLOT(0.,0.,999)
      STOP
      END
```

```
      SUBROUTINE PGRAD(C1,C2,XC,YC,VAL1,SUMX,SUMY,PGRADX,PGRADY)
      PGRADX = C1*((XC/VAL1)+SUMX)+C2
      PGRADY = C1*((YC/VAL1)+SUMY)
      RETURN
      END
```

VITA

Walid Jubran Esmail was born in Bireh, Palestine on February 22, 1946, the son of Jubran and Handumeh Esmail. He completed all his pre-College education at Friends Boys School in Bireh, Jordan, where he graduated in June, 1965. In September, 1967, he enrolled at Southeastern Louisiana College, Hammond, La. In September, 1968, he transferred to Louisiana State University, from which he received the Bachelor of Science degree in Petroleum Engineering in May, 1971. In January, 1972, he enrolled in the Graduate School of Louisiana State University to begin work toward the Master of Science degree in Petroleum Engineering.